Department of AERONAUTICS and ASTRONAUTICS
STANFORD UNIVERSITY

SMALL SCALE LUNAR SURFACE PERSONNEL TRANSPORTER EMPLOYING THE HOPPING MODE

ANNUAL REPORT OF NASA GRANT NGR-05-020-258

PERIOD MARCH 1, 1968 TO FEBRUARY 28, 1969

MAY
1969

The work described in this report is supported by
National Aeronautics and Space Administration under
NASA Grant NGR-05-020-258

SUDAAR
NO. 377

Department of Aeronautics and Astronautics
Stanford University
Stanford, California

SMALL SCALE LUNAR SURFACE PERSONNEL TRANSPORTER EMPLOYING THE HOPPING MODE

ANNUAL REPORT OF NASA GRANT NGR-05-020-258
PERIOD MARCH 1, 1968 to FEBRUARY 28, 1969

MAY 1969

SUDAAR NO. 377

NASA Coordinators: M. Sadoff
W. Larsen

Faculty Sponsors: H. Seifert
D. DeBra
J. Manning

Research Assistants: R. Degner
H. Adelman
J. Jones
R. Meetin
S. Pasternack
S. Peterson

The work described in this report is supported by
National Aeronautics and Space Administration under
NASA Grant NGR-05-020-258

TABLE OF CONTENTS

		Page
LIST OF ILLUSTRATIONS	. . . . .	
CHAPTER		
I	INTRODUCTION AND SUMMARY	1
II	HUMAN FACTORS IN HOPPING LOCOMOTION	6
III	TERRESTRIAL DEMONSTRATOR FOR HOPPING LOCOMOTION	7
IV	PROPULSION FOR THE LUNAR POGO	16
V	TERRESTRIAL DEMONSTRATOR PROPULSION	20
VI	STABILIZATION AND CONTROL FOR THE LUNAR HOPPER	27
VII	SYSTEM DESIGN	35
VIII	SOIL MECHANICS AND FOOT DESIGN	38
IX	CONCLUSION	43
REFERENCES	. . . . .	44
APPENDICES		Page
A	EQUATIONS FOR THE INITIAL AND FINAL PRESSURES THAT MUST BE ACHIEVED IN THE CYLINDER	45
B	TEMPERATURE-PRESSURE-MASS RELATIONSHIPS FOR GAS TRANSFER BETWEEN GAS RESERVOIRS	51
C	COMPUTER MODEL OF LUNAR POGO PROPULSION DYNAMIC OPERATING CYCLE	58
D	OPTIMUM PISTON DISPLACEMENT RATIO	63
E	PROPULSION ANALYSIS SYMBOL DEFINITIONS	64
F	ANGULAR OFFSET ϵ REQUIRED TO PROVIDE $\dot{\theta} = 0$ AT $\theta = 0$ UPON LANDING	67
G	CALCULATION OF CONTROL MOMENTS FOR TYPICAL LUNAR HOP . .	68
H	CONTROL THEORY, LIST OF SYMBOLS	72

LIST OF ILLUSTRATIONS

Figure		Page
1	First-Order Model of Lunar Pogo	3
2	Schematic Hop Sequence for Fixed Leg Design	5
3	Acceleration Test Facility	6a
4	Demonstrator Propulsion System Profile View	8
5	Demonstrator Propulsion System Plan View	9
6	Demonstrator Propulsion Schematic	10
7	Demonstrator Pressure-Time History	11
8	Demonstrator Stabilizing Gyro (From Norden Bomb Sight)	13
9	Demonstrator Configuration Mock-Up	14
10	Demonstrator Landing Leg Geometry	15
11	Pogo Gas Parameter Cycles on Level Terrain	17
12	Pogo Gas Parameter Cycles on Rolling Terrain	18
13	Velocity Leg Orientation on Landing	28
14	Schematic Twin-Gyro and Coordinates	30
15	Pitch Axis Controller Schematic	32
16	Roll and Yaw Axis Controller Schematic	33
17	One-Man Hopper - Artists Conception	36
18	Pogo System Block Diagram	37a
19	Cleat Configuration	40
20	Soil Impact Simulator	42
21	First-Order Trajectory	46
22	Acceleration Segment of First-Order Trajectory	47
23	Gas Flow Between Two Reservoirs	52

Figure Page

24 Control Volumes for Gas Flow Between Two Reservoirs 53

25 Flow Chart for Hopping Cycle Parameters 60

26 Root Locus 70

I. INTRODUCTION AND SUMMARY

The present program is primarily concerned with the analysis and design of a transporter to be used by Apollo astronauts to extend their operating range on the moon. Goals of the program are to design a one-man transporter with the following characteristics:

1. maximum gross weight from 1000 to 1200 pounds fully loaded
2. payload of approximately 80 pounds (excluding pilot and his life support system) when fully fueled
3. minimum operating range of 10 miles

In the course of examining the problem of mobility on the Moon, the question arose whether it should not be possible to take advantage of the weak lunar gravity and leap from one point to another. Leaping, however, should not be by rocket with its excessive propellant consumption, but by pressing against the lunar surface with a foot, after the manner of certain terrestrial creatures such as the kangaroo, rabbit, and frog. A terrestrial demonstrator of the basic "hopper" is now being built and is described in Section III. The following status report summarizes one years work on such a demonstrator and also on the ultimate lunar system the "Lunar Pogo", under NASA Grant NGR-05-020-258. Basic characteristics summarized below also appeared in semi-annual report SUDAAR 359.[5]

Ballistics: Hopping is well adapted to the low lunar gravitational acceleration of 5.31 ft/sec^2. At 45° elevation launch, a velocity of 15 ft/sec results in a horizontal leap of 50 ft in 4 sec, with a maximum horizontal capability[1] of 10.7 ft/sec or 7.3 miles/hr. Similarly[2], a launch velocity of 42 ft/sec yields leaps of 420 ft in 14.3 sec, and a maximum speed of 28 ft/sec or 19 miles/hr. Pauses between leaps will of course decrease the average speed. In the event that a given landing area may be found to be unsatisfactory – a crevasse or a large rock, for example – a fail safe or abort capability can be provided by adding a relatively light rocket system. A 1200 lb vehicle executing 50 ft. hops can for example be stopped dead in mid-flight by a rocket ejecting less than 2 lbs. of propellant at I_{sp} = 200 sec.

Human Factors: The first and most important question to be considered in a manned hopping transport system is of course "Can the pilot take it?" Previous work on human tolerance to acceleration[3] relates mainly to steady acceleration (centrifuges) or single impulses (ejection seats). Experiments to investigate how well a man can tolerate the repeated accelerations necessary for a hopping trip are described in Section II. A 10-mile trip might require one thousand 50-foot leaps, involving average accelerations of 3 g's lasting a total (decel plus accel) of 0.3 seconds each and separated by about 3 seconds of free-fall flight. It would of course be both possible and highly probable that rest or exploratory stops would be made at frequent intervals.

In the absence of firm human tolerance data, the Pogo vehicle has been sized for average accelerations of 3 g over 0.3 second. The natural thrust-time function produced by a fixed mass of expanding gas is an instantaneous 5g decreasing rapidly to 1g over 0.15 second. This "spike" of acceleration will probably be blunted by the compliance of the system (and the pilot), and could be tailored to any desired shape by suitable gas valving and adjustment of acceleration distance.

Propulsion: Propulsion is accomplished by expanding gas against a piston (Fig. 1). This propulsion system performance, analogous to that of a steam engine, depends on the mechanical work done by a working fluid, rather than on the momentum of a propellant, as with a rocket. Hopping motion is largely conservative, in that the majority of the gas expansion work done at launch may be recovered by gas compression upon landing. Fuel consumption is low; a ten-mile excursion of a 1-man, 1200 lb vehicle should be accomplished with the expenditure of 50 lbs. of N_2 at ambient temperatures, or 10 lbs. of N_2H_4 decomposed at 2000°F. The propulsion system must meet the novel requirement that each individual leap be tailored to the terrain. Leap length, and up or down hill slope, all affect the required piston pressure and hence the gas mass used.

Stabilization: It is essential that a manned hopping vehicle maintain a prescribed attitude at all times. A preliminary review of human factors and structural problems indicates that a better design results if one does not attempt to maintain the pilot continuously upright, but during acceleration and deceleration rotates him and the vehicle so that acceleration

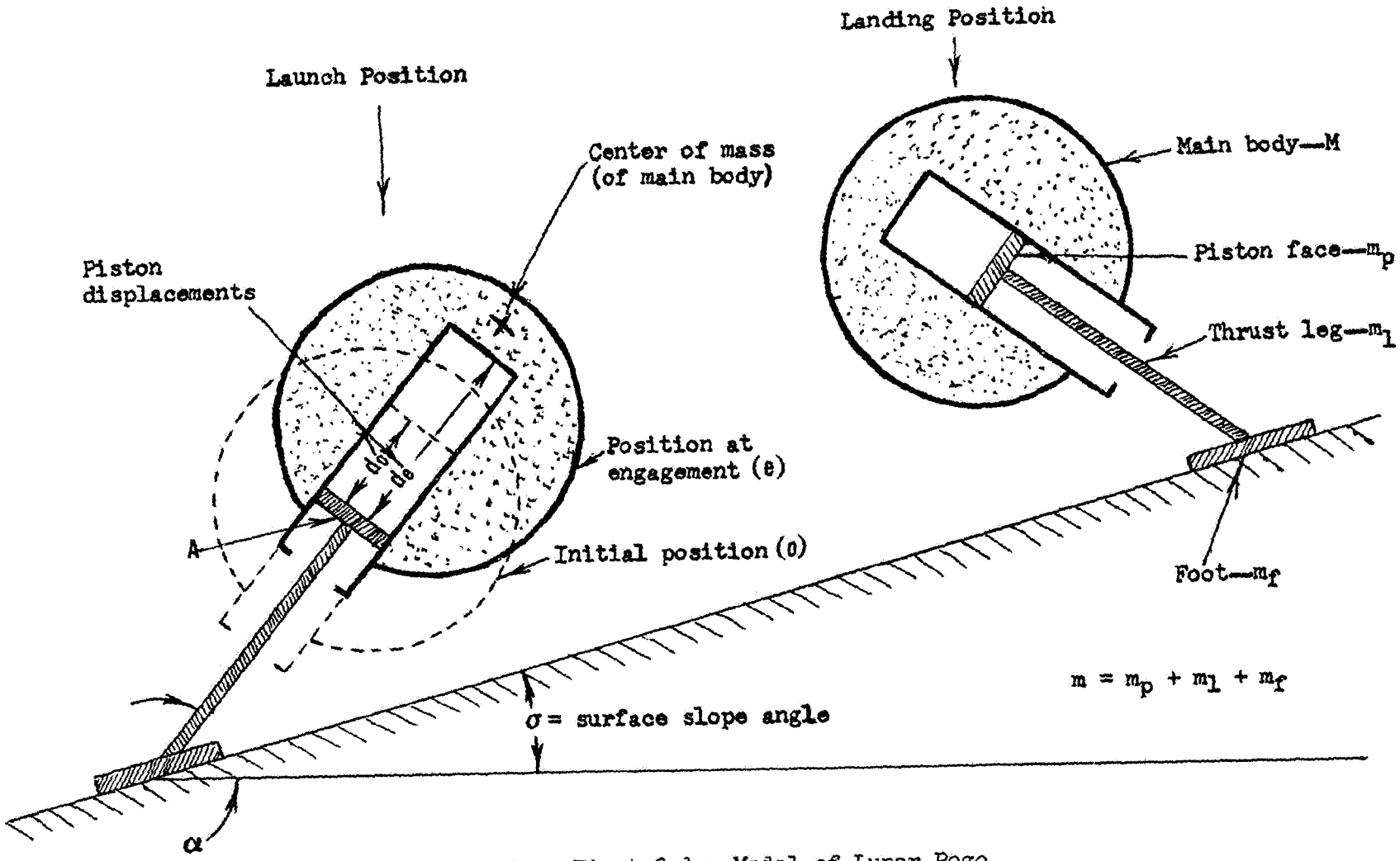

Figure 1. First-Order Model of Lunar Pogo

vectors have a fixed orientation relative to his body (Fig. 2). This attitude control can be accomplished by paired gyroscopes whose mass is approximately 20% or less of the systems mass.

Control: It will be necessary for the pilot to identify a suitable landing point and supply the control system with its coordinates, in order that a proper launch velocity and elevation be set into the system. The optics, electronics, servos and computer logic needed to do this have not yet been designed. It has been assumed for the present that these components will be within the state of the art. It should be mentioned that a vehicle capable of 50 ft. horizontal hops is also capable of 30 foot vertical reconnaisance hops in situ, during which the terrain can be scanned for suitable landing sites. This same vertical capability could be used in negotiating step-like differences in level.

Lunar Surface Reaction: Launch at 45° requires a horizontal traction force equal to the vertical force of the launching "foot". The design of a properly sized and cleated foot to supply these forces is difficult without more knowledge of the lunar surface material, which it is hoped will be available soon. A launch angle greater than 45° from horizontal can always be found which will limit the required horizontal traction force component to whatever the soil can provide. The possible presence of rocks of a size comparable to the "foot" is also a source of problems. The philosophy adopted in the design of the foot is that it will be possible within limits for the astronaut to choose his path so that unacceptable obstacles are avoided, as is often the case in terrestrial exploration. Because of the absence of soil data, a simple experiment is being designed in which cleats can be impacted and launched from sand beds, to give insight into skid and other aspects of soil behavior under transient loads.

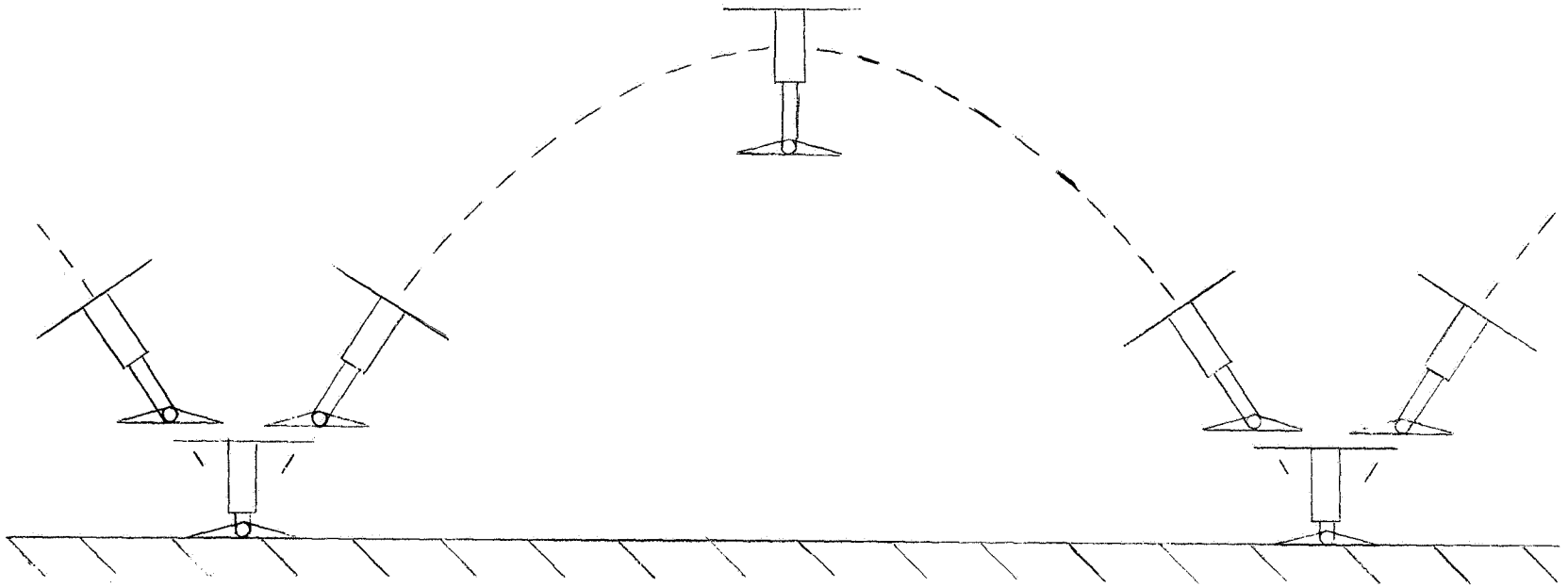

Figure 2. Schematic Hop Sequence for Fixed Leg Design.

II. HUMAN FACTORS IN HOPPING LOCOMOTION

The setup for testing human acceleration tolerance is pictured in Fig. 3, and operates as follows: 1) an electric motor-driven drive train reels in a cable which lifts the seat to a maximum height of 6 ft in 5 to 12 seconds; 2) an electromagnetic clutch then disengages the spool from the drive train allowing the seat to accelerate downward under the influence of gravity, and 3) as the seat approaches the ground, it is rapidly stopped in a distance of 2-1/2 ft or less by the action of shock absorbers mounted on either side of the seat frame. Hydraulic cylinders have been modified to act as shock absorbers. Variable restrictions in the fluid lines allow the acceleration forces which stop the seat to be varied. Gearing in the drive train permits this cycle to be repeated at approximate intervals of 5, 7, or 12 seconds. Accelerometers attached to the seat frame and to the test subject will be used to record accelerations.

With the test setup in its present form, the following parameters can be varied: 1) velocity at contact, 2) duration of acceleration and deceleration, 3) spacing of acceleration peaks, 4) length of cyclic run, and 5) seat inclination. It is expected that the intial phase of the testing program will involve measuring acceleration tolerance as a function of changes in these parameters. Based on these results, a decision will be made whether to modify the present test setup so that the effects on acceleration tolerance can be studied of such features as different spring-shock combinations (for changing the shape of the acceleration peaks), a seat rocking motion (to simulate reorientation of the fixed-leg pogo between and during hops), and different seating materials.

A "protocol" document is being prepared describing the circumstances of the test program in detail as they affect human subjects. A preliminary survey of the test facility has already been carried out by Dr. Ralph Pelligra, M.D., of the NASA-Ames staff. Both objective and subjective data will be gathered, and the analyses used both in component hardware design and as input to the integrated system analysis (Ref. 4, p. 20-07) which is a goal of the Pogo program.

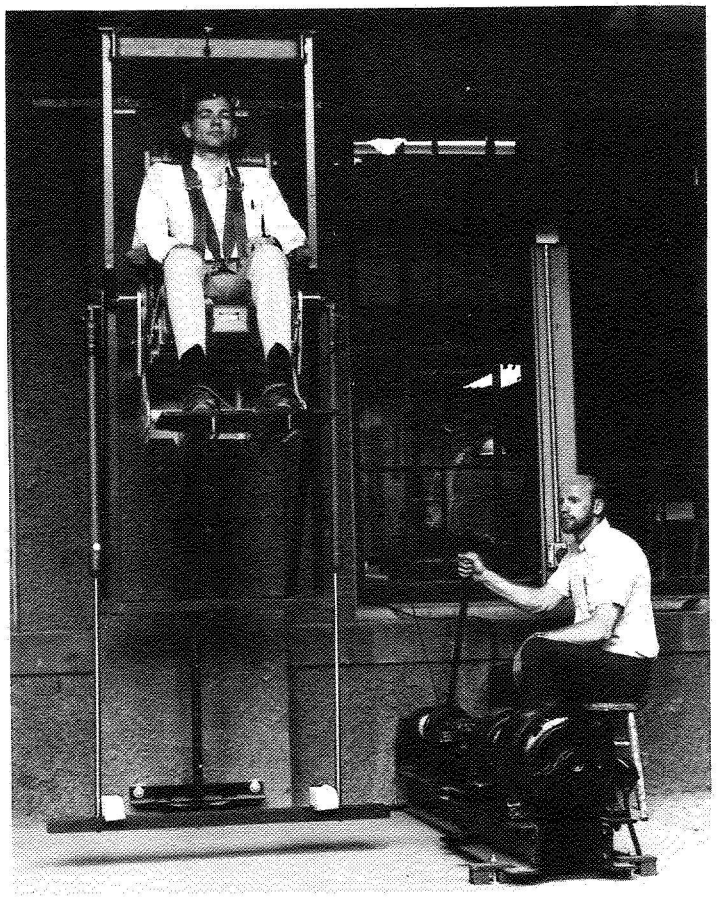

Acceleration Phase

Deceleration Phase

Figure 3. Acceleration Test Facility

III. TERRESTRIAL DEMONSTRATOR FOR HOPPING LOCOMOTION

During the contract period work was begun on a small model to be operated on the earth which would give a practical demonstration of the feasibility of the lunar hopper concept. As this is only a feasibility demonstration, the initial design specifications are set to give a simple, lightweight vehicle that will be inexpensive and easy to construct. The vehicle is to weigh approximately 50 lbs., and have the capacity of making 20 to 30 hops of about 10 feet. With this goal in mind work has begun in three major area affecting the design: propulsion, control, and structure.

A profile of the propulsion system is shown in Figs. 4 and 5, and a detailed analysis is presented in Section V. The plumbing schematic is shown in Fig. 6 and the pressure-time history in Fig. 7.

Control of the propulsion cycle probably will be a radio signal from the ground to initiate each hop. The cycle will begin when a small receiver on board receives a signal from a ground transmitter. This will trigger a timing circuit, which will make a square pulse of a predetermined length. This pulse is used to control a solenoid driver which amplifies the pulse so that it has sufficient power to move the solenoid valve. A possible alternative also being considered is making a pulse of the proper duration on the ground and sending this to the vehicle by means of a suitably modulated signal. This system has the advantage of reducing vehicle weight and making it possible to change the pulse width without approaching the vehicle. It does, however, require a slightly more complicated receiver. In either case, it is expected that the transmitter and receiver would be similar to items commercially available for use in model airplanes.

In addition to the propulsion system, an attitude control system is being developed. Because the primary purpose of the vehicle is to demonstrate the feasibility of the hopping mode of transportation, and because the ultimate 3-axis control will be complex and expensive, it was decided to make the vehicle passively stablized in a horizontal plane by means of a single strap-down gyroscope with a vertical axis. Azimuthal angle stability will be aided by a vertical tail fin. The gyro to be used

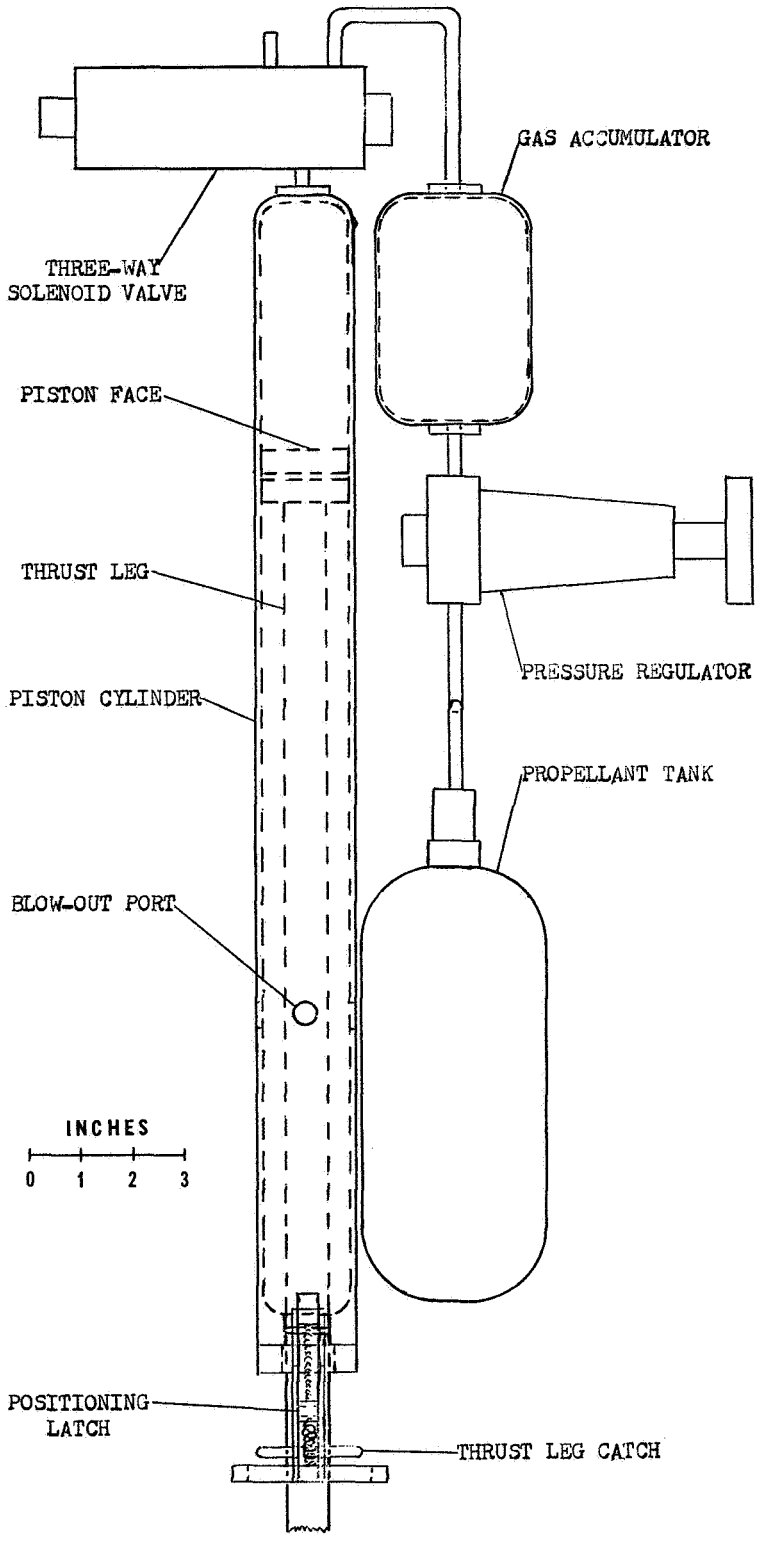

Figure 4. Demonstrator Propulsion System Profile View

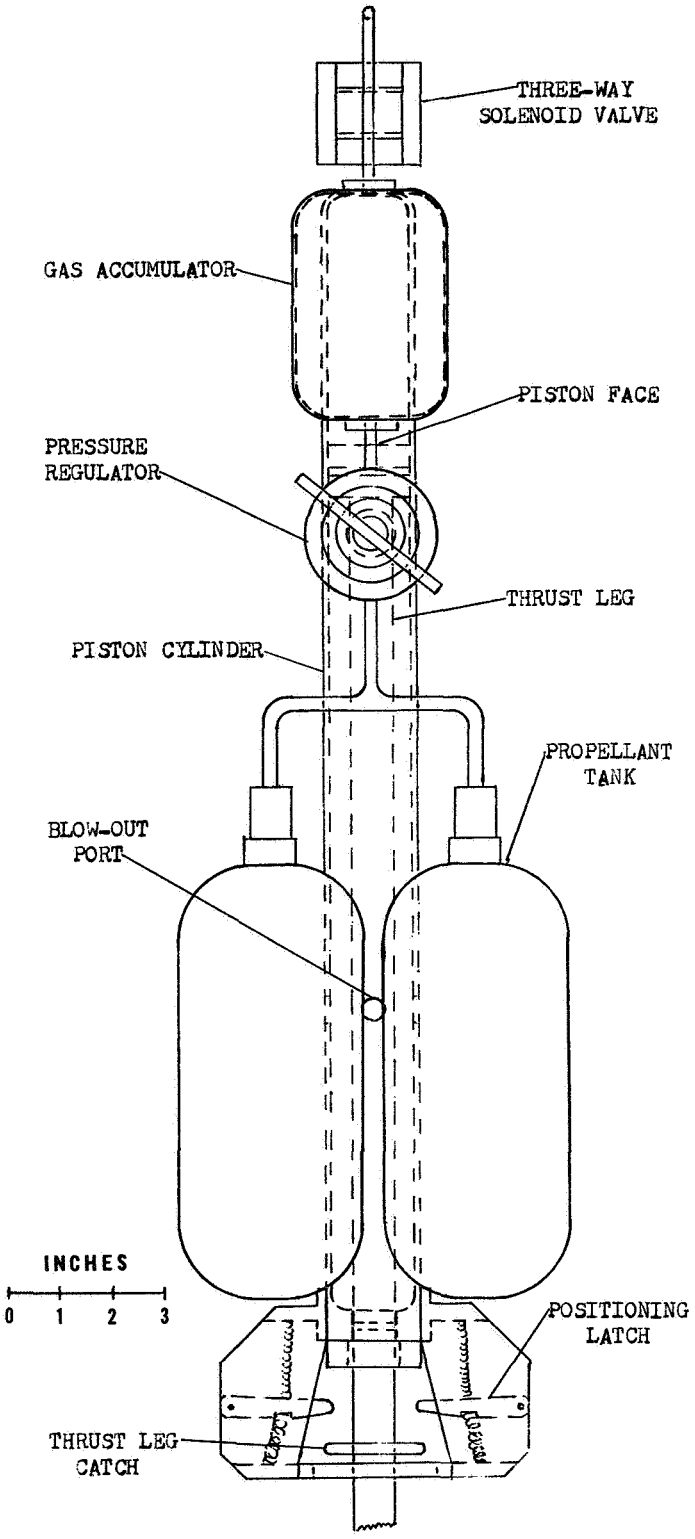

Figure 5. Demonstrator Propulsion System Plan View

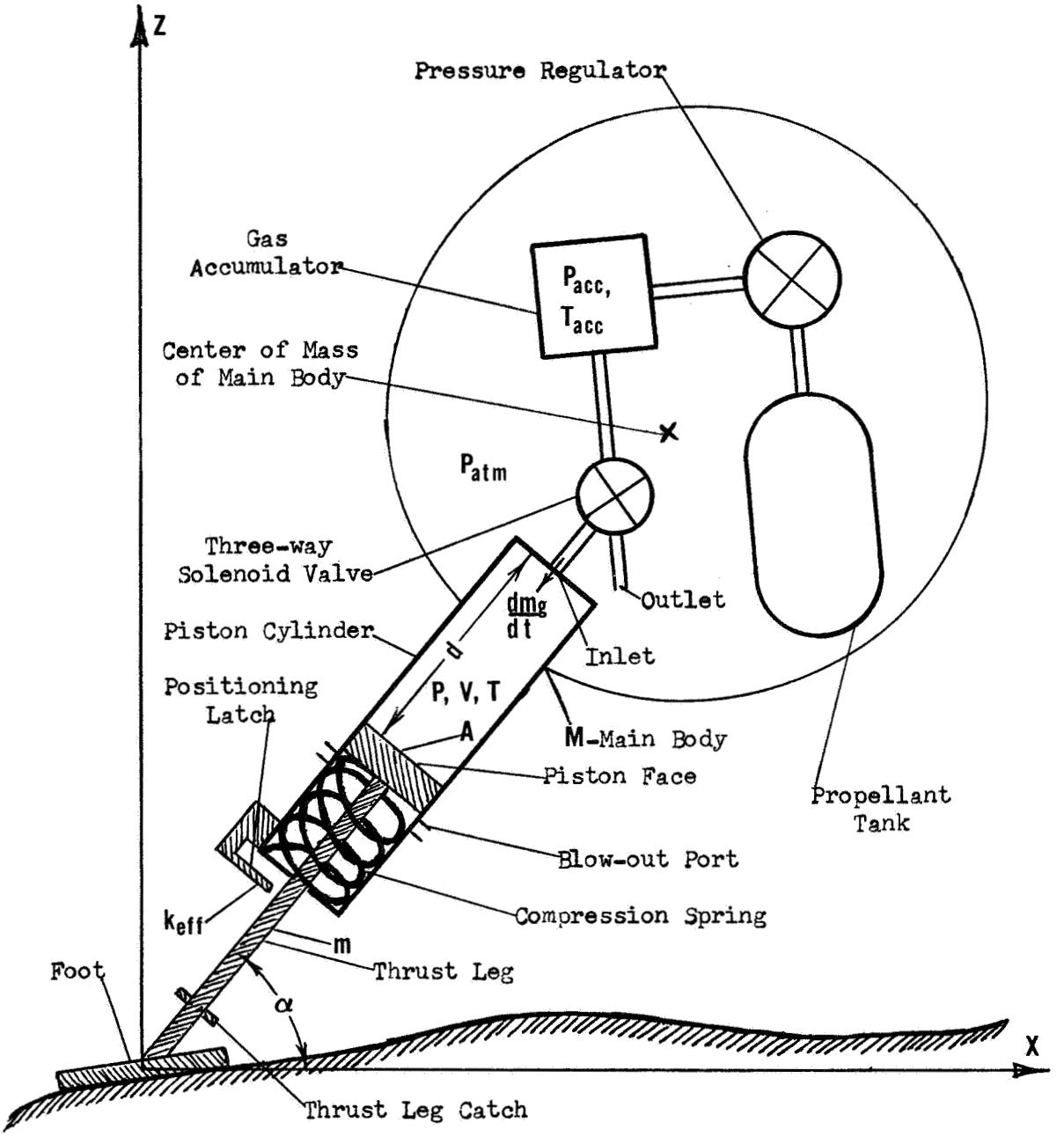

Figure 6. Demonstrator Propulsion Schematic.

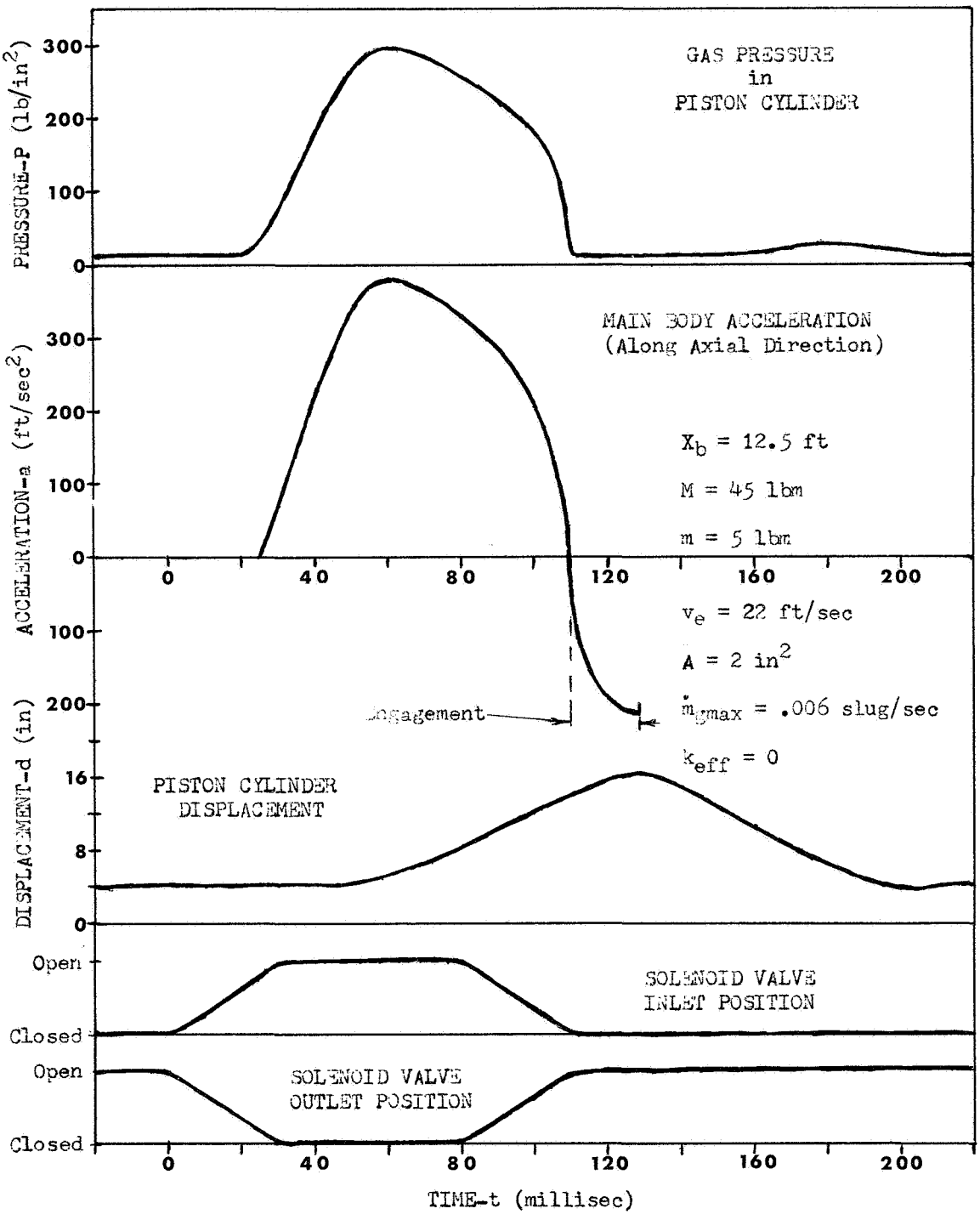

Figure 7. Demonstrator Pressure-Time History

(Fig. 8) is taken from a Norden bomb sight. It weighs 8.5 lbs.

The work done in the structures area to date has been primarily definition of the basic configuration of the vehicle. So far, this has been limited to work on the landing legs for the vehicle and relative positioning of the propulsion and control components of the vehicle.

Study of the structural configuration of the vehicle is under way. Since the landing shock will not be absorbed by the propulsion piston in this simple device, a broad tripod configuration with low center of gravity and shock absorbers in the legs will be employed. A "stick" model for study of the configuration is shown in Fig. 9.

Landing legs which resemble those of the Surveyor series spacecraft in concept are considered necessary to provide stability during landing. On the full scale craft however the control system will be sophisticated enough to handle landings on a single powered leg. In the model, with its passive control system, horizontal stability is provided by three landing legs; the base formed by these legs being wide enough that the deceleration force will not cause an over-turning moment. (See Fig. 10) To handle the condition shown in Fig. 10 is not too difficult. However, if the vehicle were allowed to rotate about its vertical axis, it would be required to accept a force whose horizontal component might possess any azimuth. This means that ideally the leg should be free to dissipate energy by moving in the direction of a landing force that can vary direction. It is difficult to build a linkage that will do this. To alleviate this problem the vehicle is to be stabilized in azimuth by the vertical fin mentioned earlier. This reduces rotation about the vertical axis and decreases the range of the approach angle, making maximum misalignment with the direction the foot travels correspondingly smaller. A search is currently underway for lightweight dampers to dissipate the kinetic energy. When these are found actual design of the leg linkage may proceed.

The centerline of the propulsion leg must pass through the center of gravity of the vehicle and must be adjustable through a 45° elevation range to cover conditions varying from vertical hops to maximum range hops.

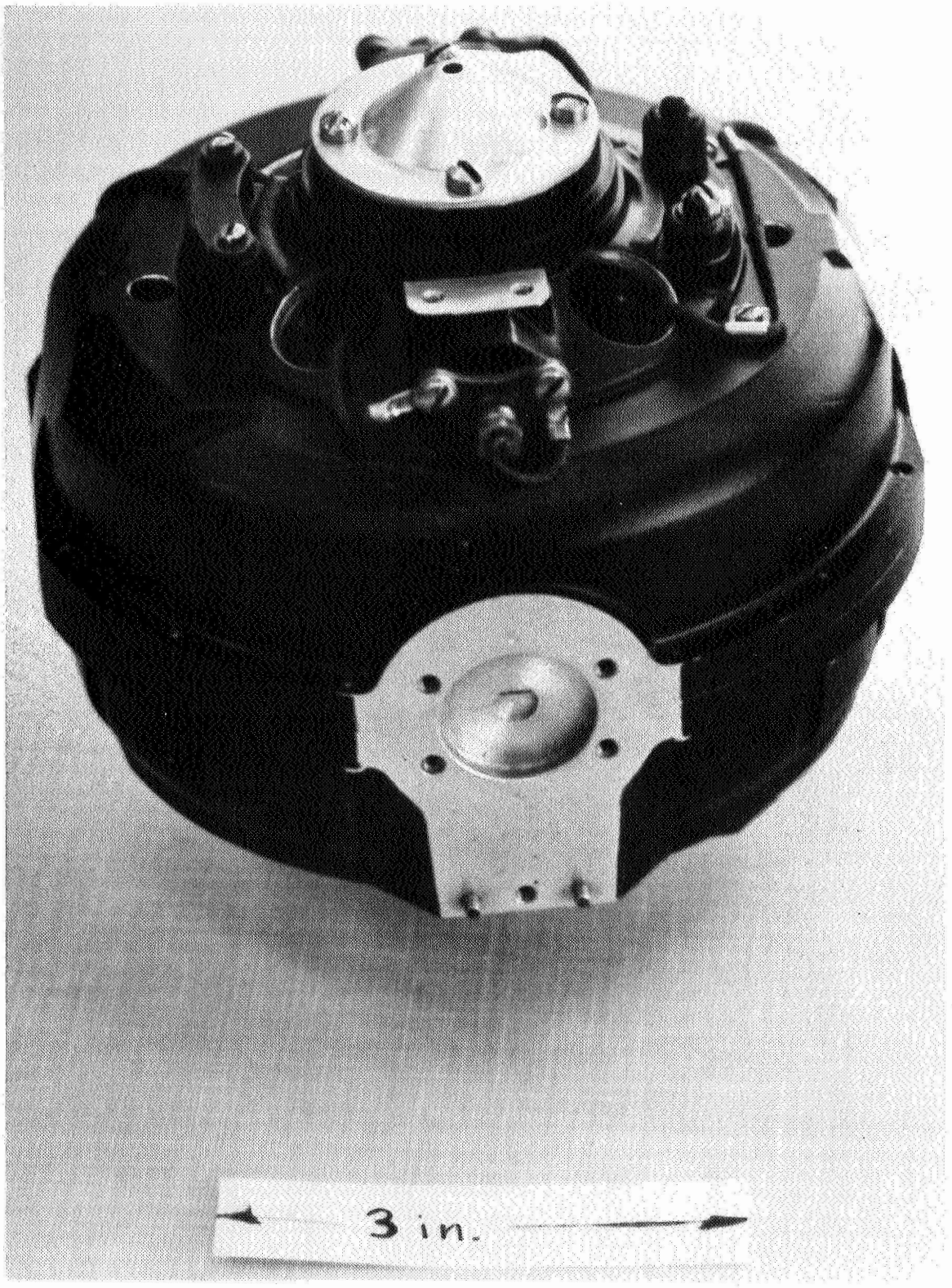

Figure 8. Demonstrator Stabilizing Gyro (from Norden Bomb Sight)

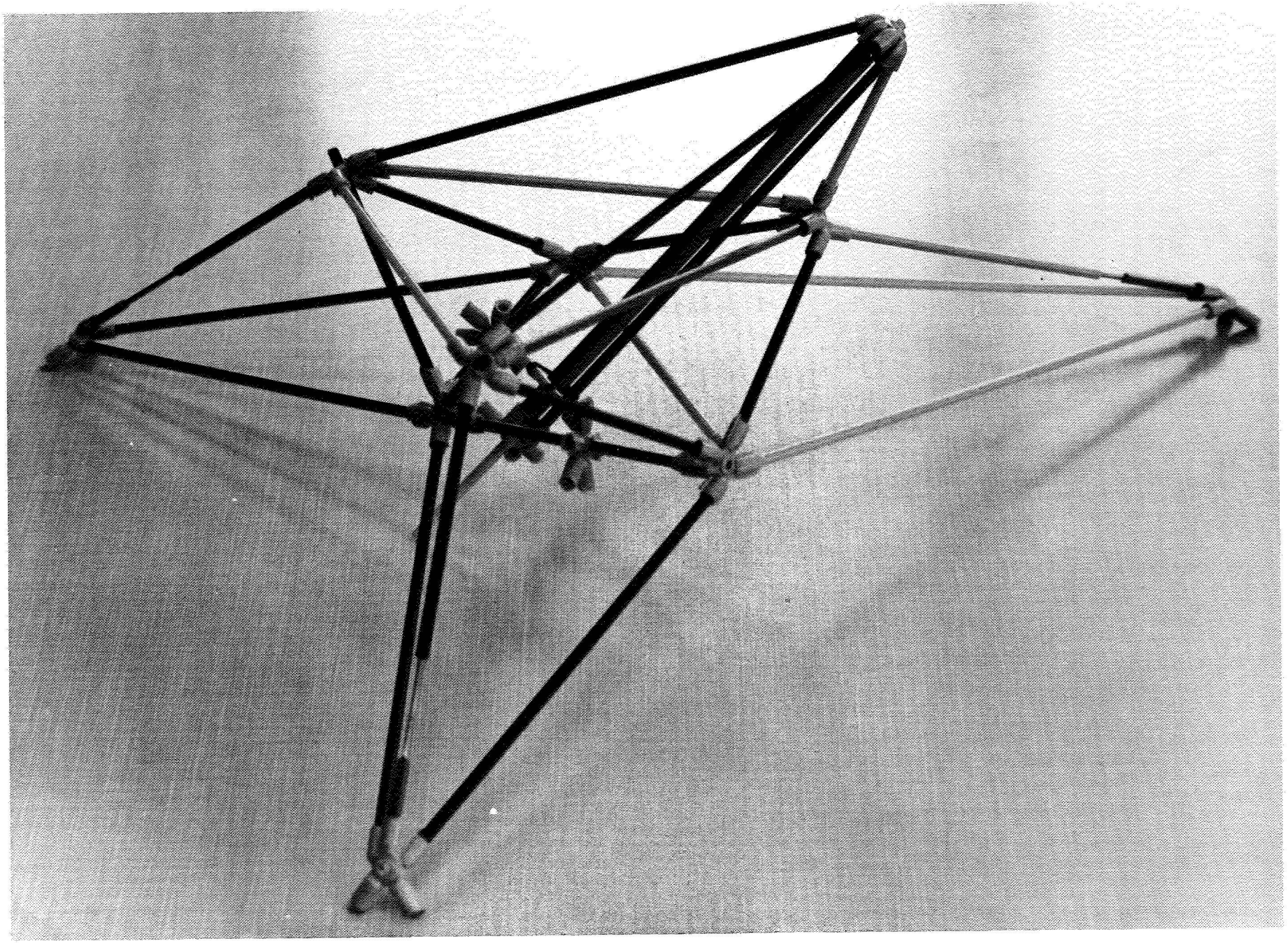

Figure 9. Demonstrator Configuration Mock-Up

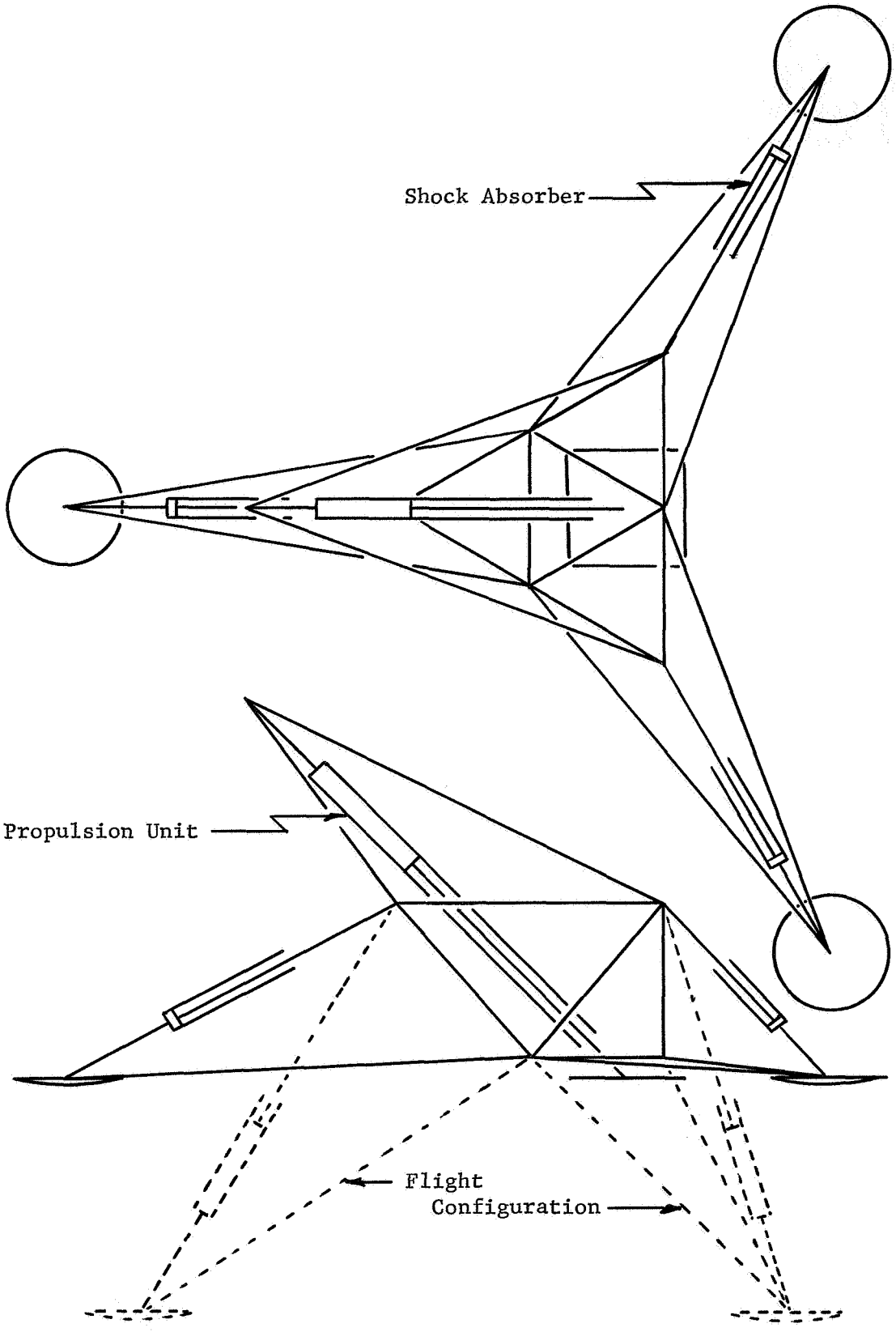

Figure 10. Demonstrator Landing Leg Geometry.

IV. PROPULSION FOR THE LUNAR POGO

The basic description of the propulsion for the Lunar Pogo is given in the Ballistics and Propulsion sections of (Ref. 5) SUDAAR No. 359, "Small Scale Lunar Surface Personnel Transporter Employing the Hopping Mode." The first-order propulsion model used is shown in Fig. 6. Preliminary analysis of propulsion is given in the Stanford University Ph.D. thesis of Dr. Marshall Kaplan, "Investigation of a Hopping Transporter Concept for Lunar Exploration", May 1968.(1)

Several relationships among the propulsion parameters were presented or discussed in SUDAAR No. 359 without derivation. In Appendix A are presented the derivations of the equations

$$p_o = \frac{(M+2m)g(\gamma-1)}{2A[1-(\frac{d_o}{d_e})^{(\gamma-1)}]} (\frac{X_R}{d_o}) \tan \alpha_{opt} \qquad (1)$$

$$p_f = \frac{Mg(\gamma-1)}{2A[1-(\frac{d_f}{d_d})^{(\gamma-1)}]} (\frac{X_R}{d_f}) \cot \alpha_{opt} \qquad (2)$$

which give the initial pressure P_o in the cylinder that must be used and the final pressure P_f in the cylinder that must be attained for a specified range X_R, optimum launch angle α_{opt}, and pairs of piston displacements d_e and d_o or d_d and d_f.

Equations determining the mass of gas which must be added or vented to the cylinder are shown in Appendix B.

To determine the quantity of propellant gas needed for the propulsion system and to see more clearly the physics of propulsion system operation, a first-order model of the operating cycle for a single hop was set up. This model made use of Eqs. (1) and (2), the equations for adding and venting gas, and the isentropic gas expansion relations. It was then extended to cover a consecutive series of hops. Figures 11 and 12 show the mass transfers and the pressure and temperature changes as the Lunar Pogo does several hops over level and hilly lunar terrain respectively. The derivation of this model is given in Appendix C.

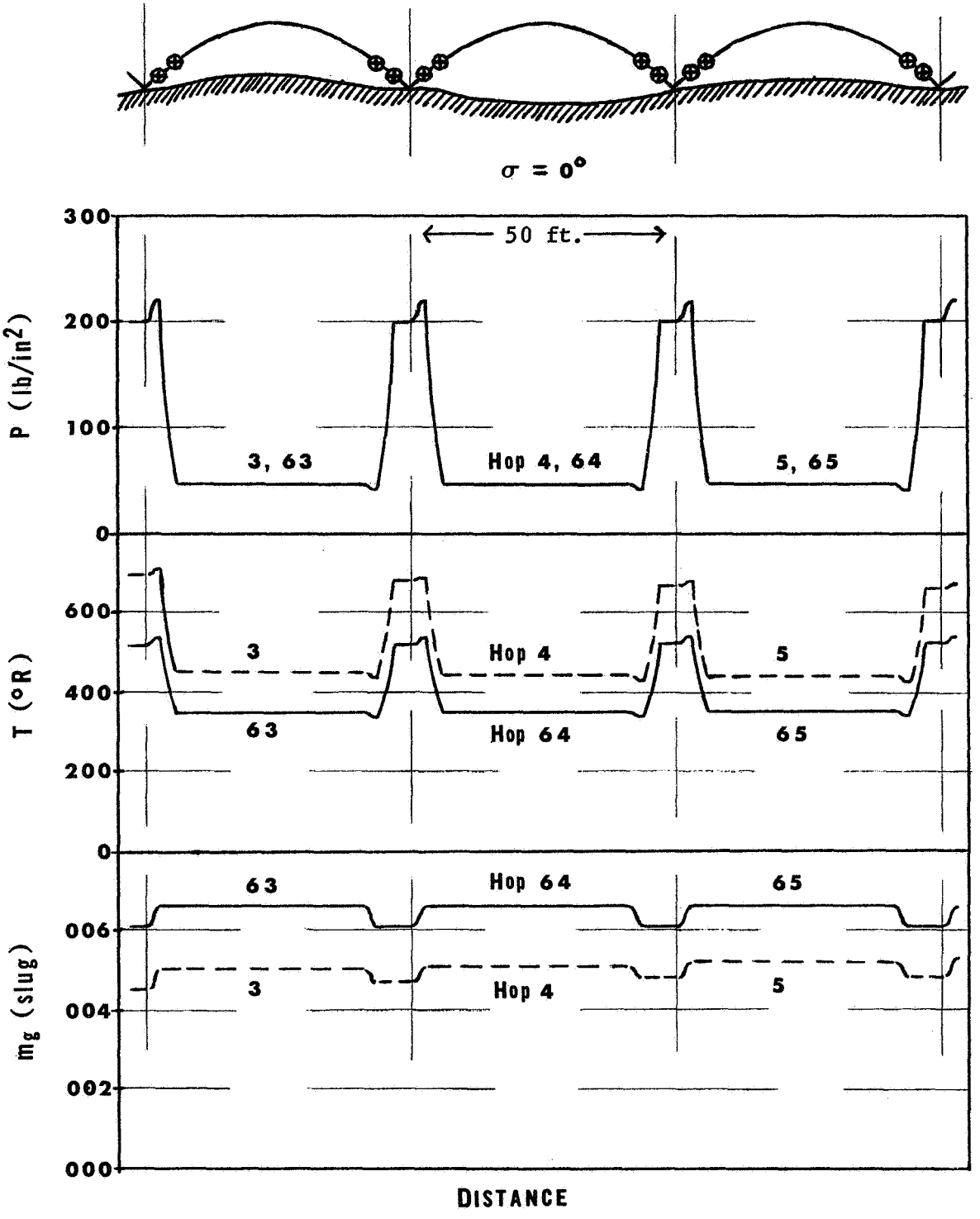

Figure 11. Pogo Gas Parameter Cycles on Level Terrain.

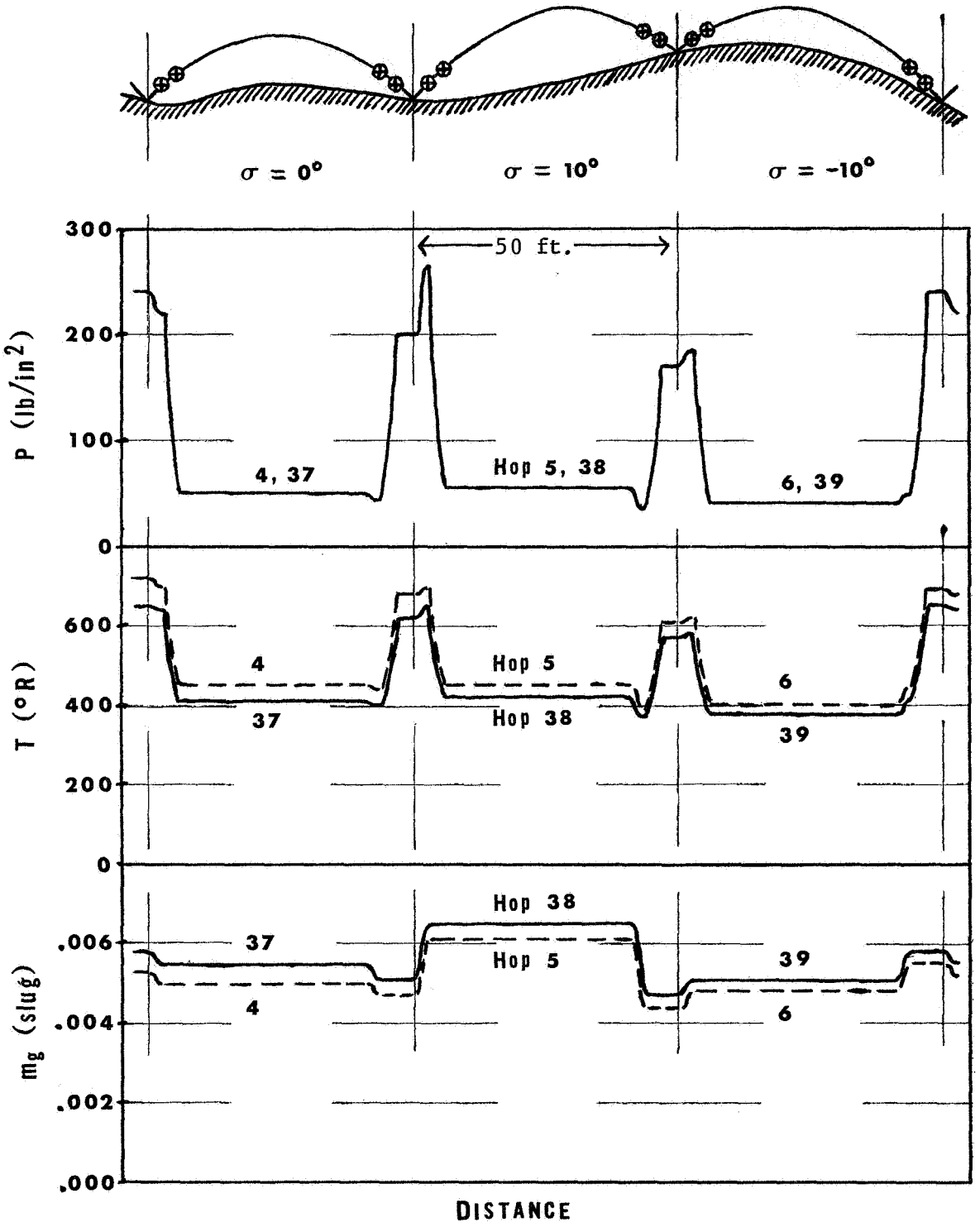

Figure 12. Pogo Gas Parameter Cycles on Rolling Terrain

Finally, Appendix D describes how the optimum piston displacement ratio $(d_e/d_o)_{opt}$ is determined.

Since the publication of SUDAAR No. 359, the semi-annual report, most effort has been on the Pogo Demonstrator. However, many of the more realistic problems of the ultimate lunar device have been identified, beyond the first-order representation in SUDAAR No. 359. These include questions such as: How can the propulsion system impart a specified velocity to the Lunar Pogo while the foot is sliding or adhering to the surface? Is some sort of velocity feedback system needed during acceleration? If gas must be added to or vented from the piston cylinder at the beginning of deceleration to achieve a proper landing, what must be the response time and flow capacity of the valves that carry out the gas transfer? What are the losses due to friction and heat transfer, and how do they affect the operation cycle? Future analytical work on the Lunar Pogo will be addressed to these more realistic problems.

V. TERRESTRIAL DEMONSTRATOR PROPULSION

Introduction

The purpose of the propulsion unit in the Pogo Demonstrator is to simulate approximately the propulsion unit in the ultimate Lunar Pogo. The two propulsion units are fundamentally similar. They both employ gas expansion in a cylinder to accelerate the main body of the Pogo up a thrust leg. Basic differences between the two systems are: (1) the Demonstrator propulsion unit is designed to operate in the earth's gravity field, whereas the Lunar Pogo propulsion unit would operate on the moon in a 1/6 g field; (2) the Demonstrator propulsion unit operates only during acceleration and part of free flight – it must retract the constant orientation thrust leg to its initial (take-off) position before shock-absorber deceleration starts, whereas the Lunar Pogo propulsion unit accelerates, changes orientation, and decelerates, acting over a complete hopping cycle; and (3) to simplify plumbing, gas flows into the cylinder of the Demonstrator during acceleration, whereas the analysis of Lunar Pogo is carried out assuming no mass influx into the cylinder during acceleration.

Demonstrator Components

Figures 4 and 5 show profiles of the propulsion unit proposed for the Demonstrator. The two propellant tanks will store air at high pressure. The pressure regulator maintains the air pressure upstream of the solenoid valve at an approximately constant value, so that the mass flux through the valve can be determined. The solenoid valve is a three-way high-speed valve with a normally closed inlet port. When the valve is energized, air can flow through the inlet port into the cylinder. When the valve is not energized, air can flow from the cylinder through the outlet port to the atmosphere.

A positioning latch and thrust leg catch keep the thrust leg in its initial take-off position during the last part of free flight, during landing, and while on the ground. A metal (or air) compression spring downstream of the piston face engages the thrust leg and returns it to its initial position. If the frictional forces between the piston and cylinder

walls are too high, the compression spring may be aided by an external extension spring attached to the thrust leg, which acts in the axial direction.

Not shown in Figs. 4 and 5, but needed for the propulsion unit are a DC power supply and a timing circuit for the solenoid valve.

Operational Cycle

The propulsion unit will operate approximately as follows. Initially, the Demonstrator is on the ground. On an electrical signal from an external control unit, the timing circuit is activated. This causes the inlet port of the solenoid valve to begin opening, so that air can flow into the cylinder. The pressure in the cylinder builds up very rapidly. When the pressure force has reached a sufficient value, the thrust leg catch pushes the positioning latch to the side. The main body of the Demonstrator then accelerates up the thrust leg. About the instant the piston face passes the blow-out ports, the timing circuit causes the inlet port of the solenoid valve to close and the outlet port to open. Almost all of the air in the cylinder is vented to the atmosphere. The pressure in the cylinder drops very rapidly to atmosphere, and the main body acceleration terminates.

At this point engagement of the thrust leg to the main body begins. After the piston face passes the blow-out ports, it contacts the compression spring. It compresses the spring until the relative velocity between the main body and thrust leg is zero. This completes engagement as the Demonstrator enters free flight.

The compression spring then expands, forcing the thrust leg back up the cylinder. The thrust leg returns to its initial position, where it is held by the positioning latch for the remainder of the flight. This completes operation of the propulsion unit until initiation of another hop. For a 10-foot hop in a 1-g gravity field, the entire cycle should be completed in one second.

Demonstrator Model

To aid in making a quantitative design for the propulsion unit, a simplified model of the propulsion unit was set up. This model is shown in

Fig. 6. The significant time intervals for the model are:

$t_f \rightarrow t_o$: on ground

$t_o \rightarrow t_e$: acceleration

$t_e \rightarrow t_p$: engagement (leg pickup)

$t_p \rightarrow t_d$: free flight

$t_d \rightarrow t_f$: deceleration

The following assumptions or approximations are made for the operaticnal sequence:

1) There is no angular motion during acceleration (one-dimensional motion).
2) The positional differences between the centers of mass of the system (which includes the thrust leg) and of the main body alone are negligible for free flight.
3) The working fluid is a perfect gas ($PV = m_g RT$) with constant specific heats ($E = m_g c_v T$).
4) The gas composition is always constant.
5) The mass of gas in the cylinder is negligible compared to the main body mass.
6) The temperature and pressure of the gas in the accumulator are constant during acceleration.
7) The flow through the inlet port of the solenoid valve is always at sonic speed.
8) Body forces acting on the gas are neglected.
9) The addition of gas to the piston and the expansion during acceleration occur adiabatically and isentropically.
10) The hop is over level terrain.
11) The positioning latch has an effective force constant k_{eff} in the axial direction during acceleration.
12) The equilibrium gas relations are valid for the dynamic situation.
13) The foot does not slide during acceleration or adhere to the surface at engagement.

14) Frictional forces at the solenoid valve and between the piston and cylinder walls are neglected.

It is felt that the errors involved in making the preceding assumptions will be small, except possibly for the last two assumptions. The effects of sliding or having the foot adhere to the surface cannot be estimated at this time. During acceleration frictional losses should not affect the performance substantially, since their effect can be negated by raising the piston gas pressure slightly.

However, the effect of frictional forces may become significant during the time of thrust leg return. If this should occur, the Demonstrator would have to be altered by the addition of an extension spring (for thrust leg return), which acts during the entire period of acceleration. Use of an extension spring would not complicate the following analysis very much, but would result in greater energy losses.

During engagement and free flight, the only external force doing work on the Demonstrator is the gravitational force. From solution [Ref. 1] of the equations of motion for these intervals, the following equation results for the approximate relationship between the ballistic range and the main body velocity at the beginning of engagement: (Symbols defined in Appendix E)

$$v_e = \sqrt{\frac{g_o X_b}{\sin 2\alpha}} \left(1 + \frac{m}{M}\right)$$

Summation of forces in the axial direction during acceleration leads to the following differential equation of motion:

$$(P-P_{atm})A - Mg_o \sin\alpha - k_{eff}(d-d_o) = M\frac{dv}{dt} \qquad (1)$$

where $v = dd/dt$. As soon as the thrust leg catch deflects the positioning latch out of the way, k_{eff} goes to zero. See Fig. 6.

Use of the energy equation for a gas flowing into a cylinder of varying volume leads to the following energy differential equation:

$$V\frac{dP}{dt} + \gamma P\frac{dV}{dt} = \gamma R T_{acc}\frac{dm_g}{dt} \qquad (2)$$

where $V = Ad$. dm_g/dt represents the rate at which gas flows into the

cylinder. Equation (2) was derived from an analysis similar to that for the energy equations derived in Appendix B.

Equations (1) and (2) constitute two equations in two dependent variables d and P and in one independent variable t. They cannot be analytically integrated as far as is known. They can only be numerically integrated for various values of the parameters.

Design Criteria

The design criteria established for the Demonstrator were: (1) the weight of the propulsion unit should be no more than 20-25 lbm out of a total estimated weight of 50 lbm for the Demonstrator; (2) all components of the propulsion unit were to be made from commercially-available hardware; (3) the maximum acceleration felt by the main body of the Demonstrator during acceleration was to be no more than 15 g_o; (4) the piston travel during acceleration, (d_e-d_o), was to be no more than 1 ft; (5) the Demonstrator should be capable of making about 25 uniform hops; (6) the horizontal range of the hops should be at least 10 ft.

Hardware Sizing

Quantitative design of the propulsion unit was based on commercially available hardware and the limits to which this hardware could be stressed. The system layout is shown in Figs. 4 and 5.

The best off-the-shelf pressure vessel found that was acceptable as a propellant tank could store about 0.6 lbm of air at 2000 psi. Assuming half the air were used during a hopping sequence, the tank pressure for the last hop would be about 1000 psi. This value of 1000 psi was taken as the minimum upstream tank pressure for design purposes.

The simplest way of making each hop approximately the same is to have the solenoid inlet port open for the same length of time during acceleration and to have the pressure upstream of the solenoid the same for each hop, so that the mass influx rate into the cylinder is identical for each hop. This is done by having the timing circuit so designed as always to energize the solenoid valve for the same length of time and by having a pressure regulator upstream of the solenoid. A regulated pressure of 800 psi was selected as the pressure to be maintained by the regulator.

This pressure assures that there will always be a pressure differential across the regulator.

To have sonic flow through the solenoid inlet port, the pressure in the cylinder must be limited to about 400 psi. This pressure is then the maximum allowable pressure for the cylinder.

Another limitation on the propulsion unit was that the mass flow rate through available aerospace solenoid valves at the pressures needed was rather low.

Mathematical Analysis

To meet the design criteria, values taken for X_b, α, and M were:

$X_b = 12.5$ ft $\qquad v_e = 22$ ft/sec

$\alpha = \alpha_{opt} = 45^\circ$ (at $\sigma = 0^\circ$)

$M = 45$ lbm $\qquad \frac{m}{M} \approx 0.1$

Values used for other constants were:

$\gamma = \gamma(\text{air}) = 1.40$

$R = R(\text{air}) = 1715$ ft-lb/slug-$^\circ$R

$T_{acc} = T_{acc}(\text{room}) = 530^\circ$R

$P_{atm} = 14.7$ lb/in^2

$g_o = 32.2$ ft/sec^2

Opening and closing times of 30 milliseconds were assumed for the solenoid valve. For valve opening dm_g/dt was taken to increase linearly from $dm_g/dt = 0$ at $t = 0$ to $dm_g/dt = \dot{m}_{gmax}$ at $t = 30$ msec, and then to remain at $dm_g/dt = \dot{m}_{gmax}$ for $t > 30$ msec.

Equations (1) and (2) were then written into a computer program and numerically integrated for appropriate ranges of k_{eff}, d_o, A, and $\dot{m}_{gmax}$. Figure 7 shows a typical set of curves resulting from the numerical integration.

From an analysis of the results, the following parameter values were selected for the demonstrator design:

$d_o = 4$ in

$d_e - d_o = 12$ in

$A = 2$ in^2

$\dot{m}_{gmax} = .005$ slug/sec

Choice of the preceding parameter values will meet the design criteria, give near optimum performance, and still allow a margin for frictional losses and other losses.

Corresponding to the values chosen for d_o, d_e, A, and $\dot{m}_{gmax}$, the following additional parameter values result:

$a_{max} \approx 15\ g_o$

$t_e - t_o \approx 100$ msec

$P_{max} \approx 400$ lb/in^2

$\Delta m_g \approx .0005$ slug/hop

For 25 hops, .018 slug = .6 lbm of air must be supplied to the cylinder. Assuming leakage losses are negligible, this amount of air could be supplied by using two of the previously described propellant tanks.

The physical dimensions of the propulsion unit shown in Figs. 4 and 5 correspond closely to the design specifications that have just been given.

VI. STABILIZATION AND CONTROL FOR THE LUNAR HOPPER

A. Introduction

As presently envisioned, the pogo transporter will tip over to the desired launch angle and will be held there with an ankle brake between the leg and foot. This assumes that the foot is large enough to support the vehicle (see pg. 54-55 of reference 5, SUDAAR 359). Because the foot is locked during the acceleration phase, the vehicle should leave the surface with zero angular velocity. The control system must re-orient the vehicle to the proper landing orientation.

B. Landing Orientation

The desired landing orientation is a function of the vehicle's center of mass velocity and so it is time varying. At landing there must be an angle ϵ between the center of mass velocity vector and the leg so that some of the velocity is used to bring the vehicle to the vertical. See Fig. 13. The velocity perpendicular to the leg is $v_T = v \sin \epsilon$. The tangential velocity required to come to the vertical and arrive with zero angular velocity is $V_T = \sqrt{2g\ell[1-\cos(\theta-\epsilon)]}$. So ϵ must satisfy this equation

$$v \sin \epsilon = \sqrt{2g\ell[1-\cos(\theta-\epsilon)]}$$

Now, ϵ is small so we can approximate.

$$\sin \epsilon \overset{\circ}{\approx} \epsilon$$

$$\cos(\theta-\epsilon) \overset{\circ}{\approx} \cos\theta + \epsilon \sin\theta$$

$$v\epsilon \overset{\circ}{\approx} \sqrt{2g\ell[1-\cos\theta - \epsilon \sin\theta]}$$

$$\epsilon^2 + \frac{2g\ell \sin\theta}{v^2}\epsilon - \frac{2g\ell}{v^2}(1-\cos\theta) = 0$$

$$\epsilon = -\frac{g\ell \sin\theta}{v^2} + \sqrt{\frac{g^2\ell^2\sin^2\theta}{v^4} + \frac{2g\ell}{v^2}(1-\cos\theta)}$$

So, given v and θ at each instant, ϵ can be calculated and used as a command to the control system. This assumes there is no slippage of the foot and that the leg is of constant length during the landing. A

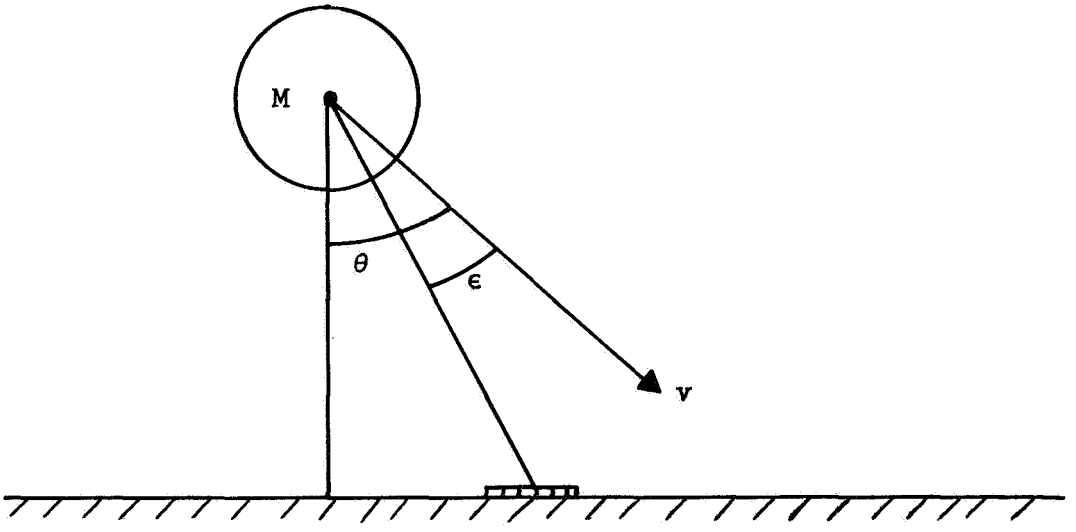

Figure 13. Velocity Leg Orientation on Landing

more nearly exact derivation is outlined in Appendix E.

C. Control System

As discussed in reference 5, SUDAAR No. 359, twin gyro controllers are being considered for the vehicle attitude control. The pertinent equations governing the motion of the vehicle for pitch plane motion are

$$I\ddot{\theta} + 2h\dot{\varphi}\cos\varphi = M_{ext}$$

$$J\ddot{\varphi} - h\dot{\theta}\cos\varphi = T$$

where θ is the pitch angle of the vehicle measured from an inertial reference direction, φ is the gimbal angle, M_{ext} is the external disturbance torques on the vehicle, and T is the control torque on the gyros. See Fig. 14. The form for T must be chosen so that the vehicle has the desired response. We can linearize these equations assuming that φ remains small.

$$I\ddot{\theta} + 2h\dot{\varphi} = M_{ext}$$

$$J\ddot{\varphi} - h\dot{\theta} = T$$

Assume that $T = k_\theta(\theta-\theta_c) + k_{\dot\theta}\dot{\theta} - b\dot{\varphi}$, and take the Laplace transform of these equations. In matrix form, we have

$$\begin{bmatrix} S^2 & \frac{2h}{I}S \\ -\left[\frac{(h+k_{\dot\theta})S+k_\theta}{J}\right] & \left(S^2 + \frac{b}{J}S\right) \end{bmatrix} \begin{bmatrix} \Theta \\ \Phi \end{bmatrix} = \begin{bmatrix} \frac{M_{ext}}{I} + S\theta(0)+\dot\theta(0)+\frac{2h}{I}\varphi(0) \\ -\frac{k_\theta}{J}\Theta_c+\left(S+\frac{b}{J}\right)\varphi(0)+\dot\varphi(0) \\ -\left(\frac{h}{J}+\frac{k_{\dot\theta}}{J}\right)\theta(0) \end{bmatrix}$$

The characteristic equation is

$$S\left(S^3 + \frac{b}{J}S^2 + \frac{2h}{IJ}(h + k_{\dot\theta})S + \frac{2hk_\theta}{IJ}\right) = 0$$

By suitably choosing b, k_θ, and $k_{\dot\theta}$ we can locate the roots of the characteristic equation to give a suitable response. Here we have considered no instrument errors or uncertainty torques about the gimbal

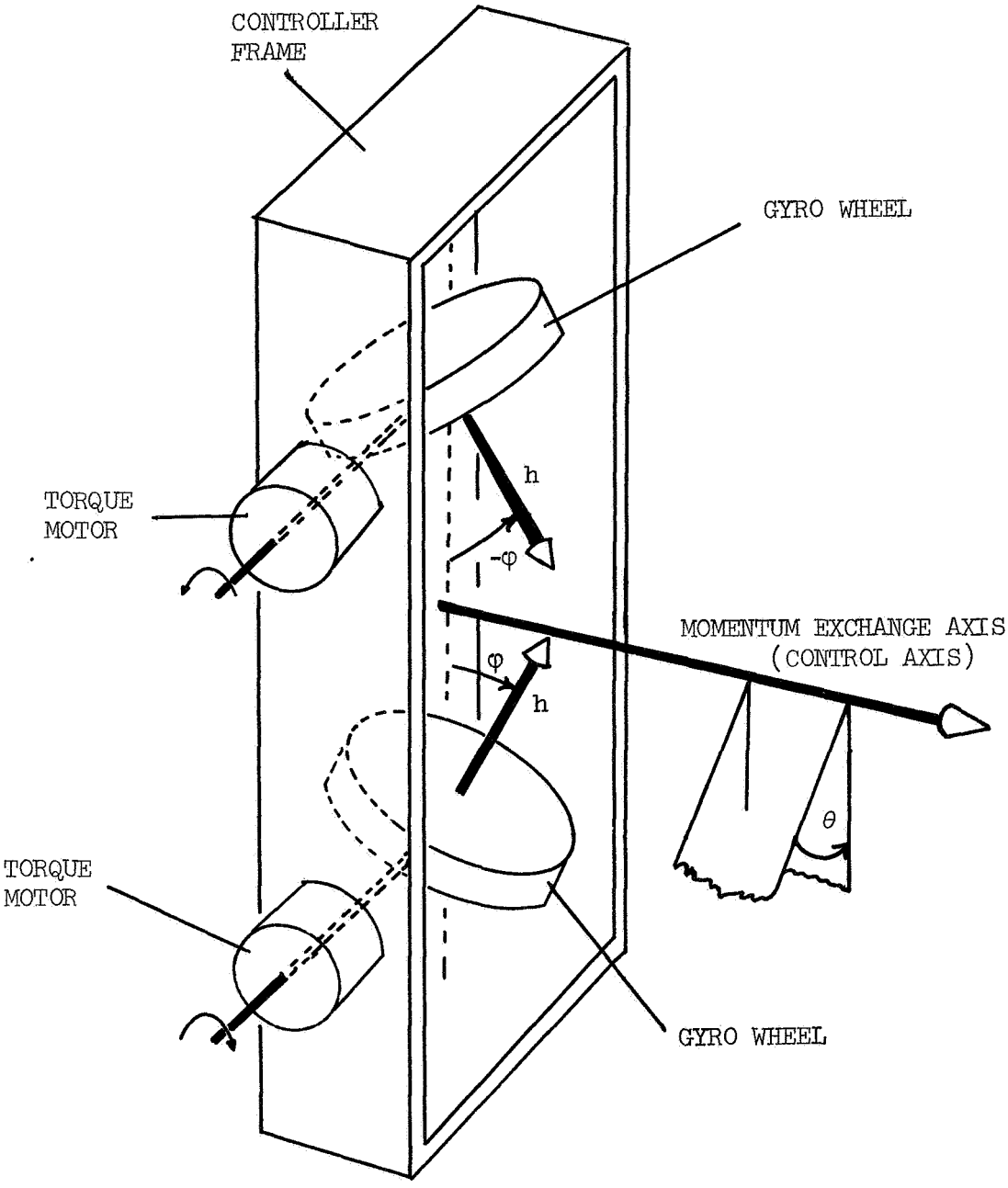

Figure 14. Schematic Twin-Gyro and Coordinates

axis. An uncertainty will cause a steady state offset in θ. This offset can be eliminated by using integral control, i.e., employing a control torque proportional to $\int\theta dt$. The gyro and torquers will have to be sized to reorient the vehicle in the allotted time of flight. A sample root locus design is shown in Appendix F. The block diagram for the pitch plane control system is shown in Fig. 15. Control about the roll and yaw axes will be similar. During flight, the roll and yaw controllers will keep the roll and yaw angles nulled. They will have to be sized to handle the gyroscopic disturbance torques resulting from the pitch rate. The block diagram for the roll and yaw axes is shown in Fig. 16. The pitch motion can essentially be decoupled from roll-yaw since roll and yaw rates will be very small and hence the gyroscopic disturbing torques about the pitch axis will be small. An example system design is done in Appendix F, using approximate values for the vehicle characteristics.

D. Mass Expulsion vs. Twin Gyro Control

The most critical phase of the flight is the re-orientation to the proper landing position. Assume we must rotate the vehicle through 90° in 4 seconds. This can be done for example by accelerating the vehicle for half the time and decelerating it the final half. The required angular acceleration is

$$\alpha = \frac{4\Delta\theta}{t^2} = \frac{4\,\frac{\pi}{2}}{16} = 0.393 \text{ rad/sec}^2$$

Assume a moment arm of 0.61 m and a vehicle moment of inertia of 407 kg-m^2. Then the thrust to produce this α must be 262 newtons. Now if a rocket were to be used,

$$F = \dot{m}c \qquad\qquad I_{sp} = 150 \text{ sec}$$

$$F = \dot{m}I_{sp}g$$

$$m \cong \frac{F \cdot t}{I_{sp}g} = .71 \text{ kg/hop}$$

Therefore, since the vehicle is designed for 1000 hops, reaction thrust would be completely unsatisfactory.

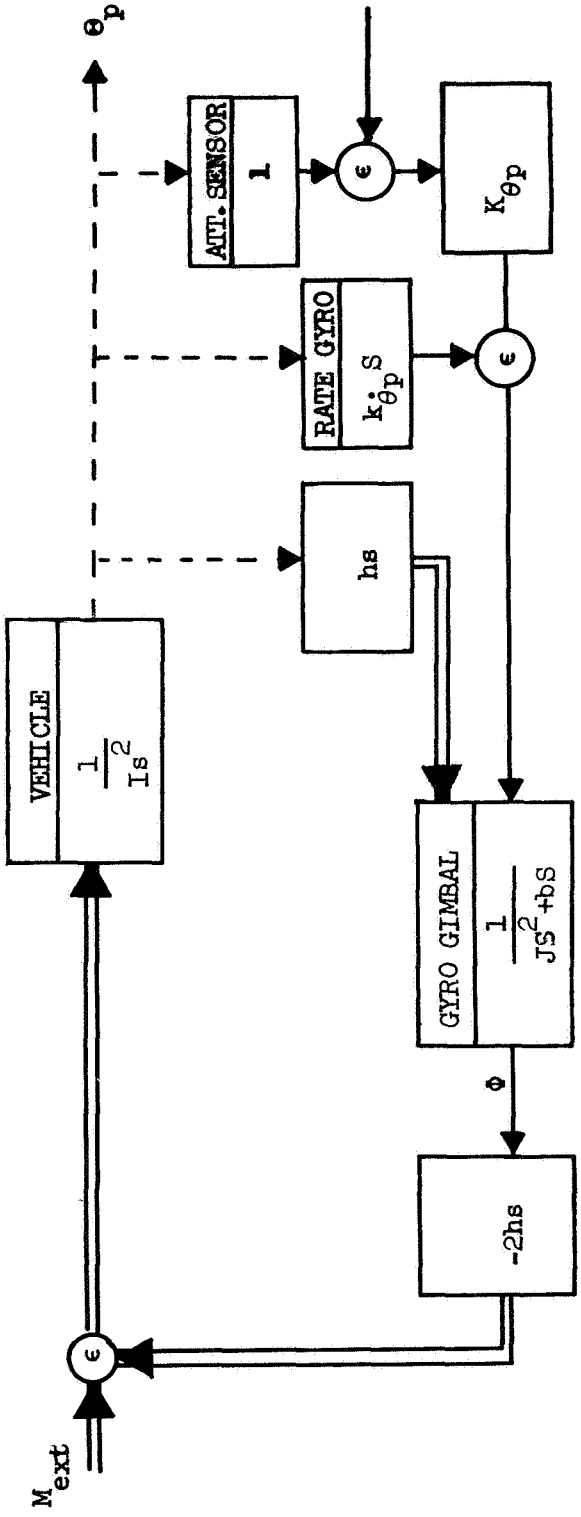

Figure 15. Pitch Axis Controller Schematic.

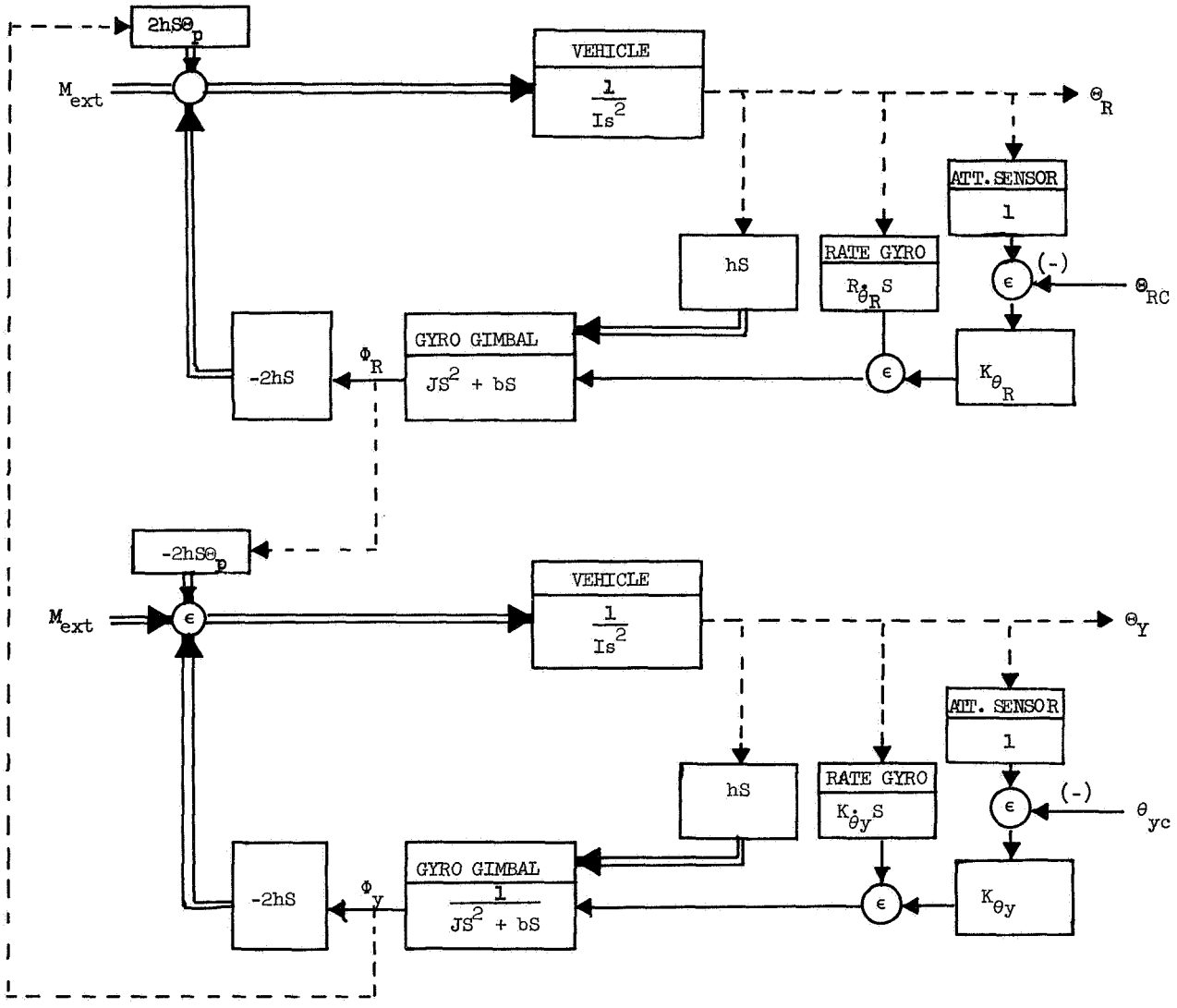

Figure 16. Roll and Yaw Axis Controller Schematic

The peak power required for twin gyro operation is of the order of 200 watts. A 4-second hop would require at most 800 watt-seconds = 0.22 watt-hours. One thousand hops require 220 watt-hours. Batteries supply (conservatively) 40 watt-hours/kg. Thus about 5.5 kg of batteries would be required.

VII. SYSTEM DESIGN

Primary attention is being focussed on a transporter in which the propulsion leg is fixed to the vehicle. The various arguments of convenience simplicity, etc., which were used in arriving at this choice instead of a swinging leg design are discussed in reference [5] pp. 9-12, SUDAAR No. 359. The motion of a fixed thrust leg vehicle is shown diagrammatically in Fig. 2. Figure 17 shows an artists rough sketch of how such a design might appear in flight.

An overall quantitative systems analysis and optimization will require a mathematical model of each of the subsystems, such as propulsion, stabilization, and structures, each of which should incorporate a scaling law for the weight of important components. The state of the development of the subsystems does not yet permit defining mathematical models, but it is anticipated that more rapid progress will occur after current work on the terrestrial demonstrator is completed.

A lunar hopping vehicle resembles a missile system in that weight plays an important role. It is necessary therefore to evaluate design trade offs carefully to secure a final configuration with minimum weight. Owing to the complex interactions among various pogo parameters, separate optima for each subsystem will not ensure an optimum design for the overall system.

One method for achieving overall system optimization is to use a "generalized design analysis". Quoting from reference [4] page 20-07, a description of such a method as applied to a missile follows: "A generalized design analysis provides a unified study of self-consistent conditions in which all the factors are allowed to interact properly with one another. This analysis consists of a formulation of features such as component weight of the missile structure, hydraulic system, engine, pressurizing systems; the environment conditions of the atmosphere; the geometric aspects of size, shape, number of stages, and position of components; and the physical properties of densities, allowable stresses, specific heats, and vapor pressures."

"The design and performance of the missile system are determined by interactions between these factors consistent with the physical laws

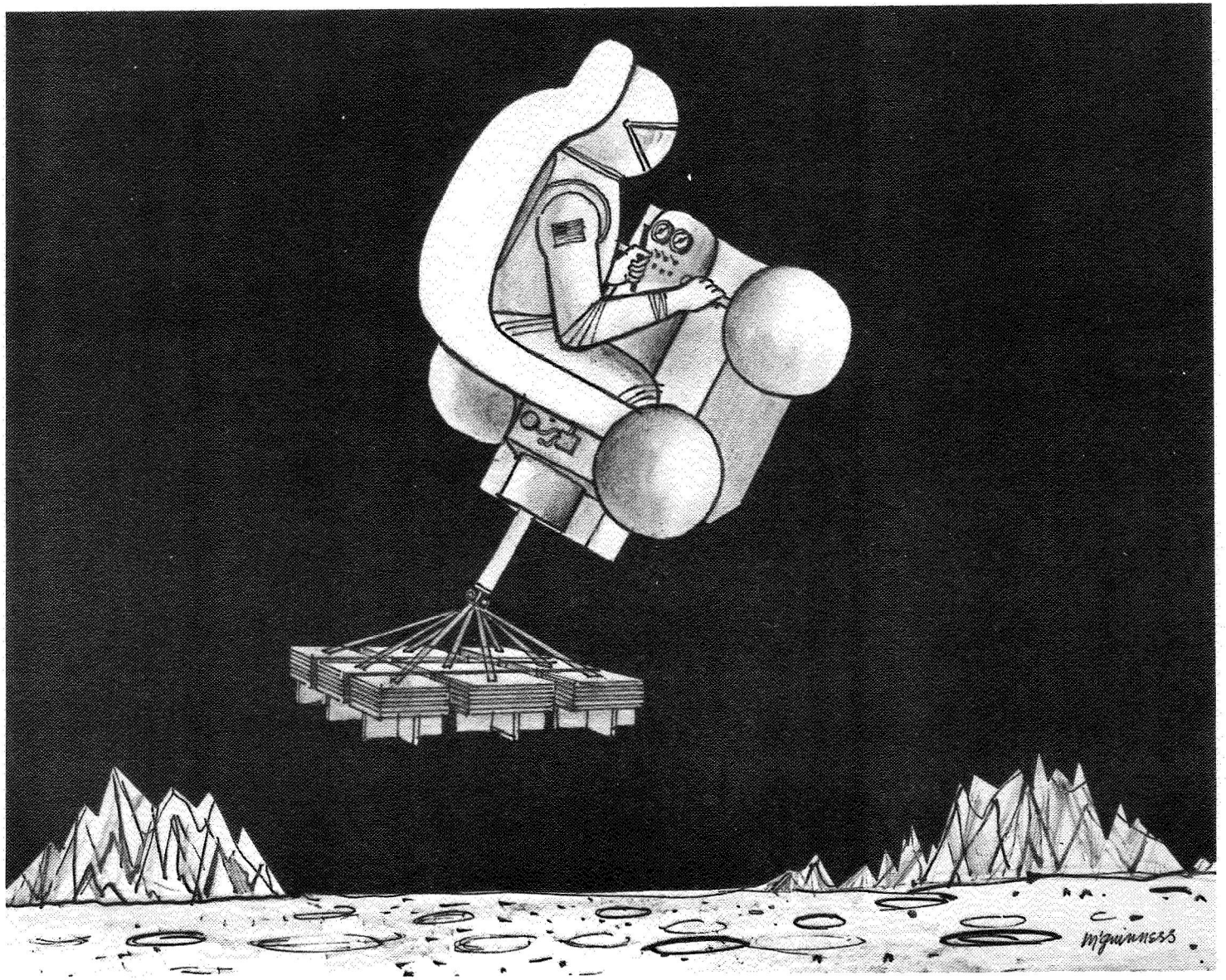

Figure 17. One-Man Hopper – Artist's Conception

governing trajectories, aerodynamics, thermodynamics, material failure, radiation, etc., and are subject to the constraining conditions of pump pressure margins, minimum thicknesses, mixture ratios, etc."

"The basic technique of the analysis is the reduction of detailed analysis of the complete complex system to a few relatively simple component relationships that react with one another. The component analyses are coupled together, the "output" of one serving as "input" to others, in sucha a manner as to close the loop for the system. Because of the complexity, programming on a digital computer is required."

"The analysis is established in a manner that allows introduction of adjustable parameters such as allowable stress, minimum gage, slenderness ratio, etc., as inputs to the system. As the vehicle "flies" in the computer, certain variables, such as skin gage, bending moments, pressures, etc., are computed at each instant of flight so that the vehicle designs itself as it moves along consistent with the conditions and constraints of the analysis."

Although the component analyses for the pogo system will differ from those of a missile system, a basic computer program for carrying out the analysis would be similar. Previous successes with the use of this type of analysis on missle systems and the inherent similarities between the missile and pogo systems indicate that a substantial contribution to the pogo system design would result from an analysis of this sort.

Figure 18 is a flow chart which gives an approximate idea of the component analyses which must be carried out and their mutual interaction. As specific quantitative component analyses are carried out, refinement of the overall systems analysis can take place.

The following outputs can be expected from this analysis: 1) preliminary size and performance estimates for different vehicle configurations, 2) specific information for detail design parameters such as cylinder wall thickness, gyro sizes, and weights of various components which are otherwise difficult to determine owing to strong interactions, and 3) exchange ratios for the effects on overall performance of such parameter changes as an increase in payload, decrease in maximum acceleration which can be tolerated by the pilot, or decreased launch angle required to prevent slippage of the foot.

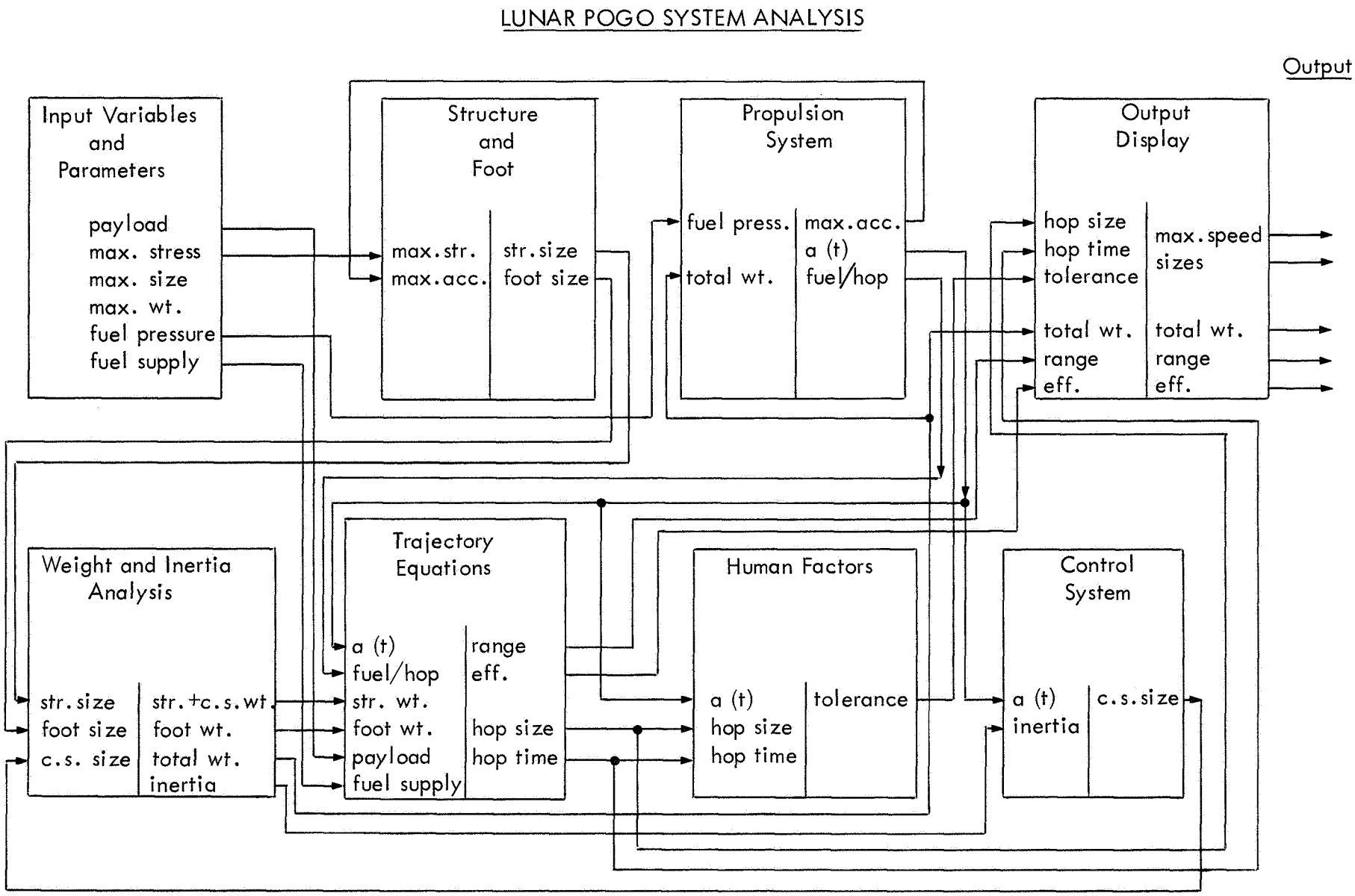

Figure 18. Pogo System Block Diagram.

VIII. SOIL MECHANICS AND FOOT DESIGN

As was discussed in some detail in the semi-annual report, SUDAAR No. 359, the lunar pogo device will operate most efficiently at take-offs 45° to the surface. To permit this departure angle the coefficient of friction between the lunar surface and the pogo foot must be at least 1.0. The tractive effort, or maximum shearing force, developed between a soil and a flat plate on its surface is given by the formula

$$H = W \tan \varphi + Ac$$

where W is the weight on the plate, A is the contact area with the surface, c is the coefficient of cohesion of the soil, and φ is the "angle of friction" of the soil.

The Surveyor landings have provided data on the cohesive and frictional properties of the lunar soil. φ is approximately 35° and c is 0.07 psi which indicates little cohesiveness. For these values,

$$\frac{H}{W} \cong \tan \varphi = 0.7$$

which appears too small permit 45° take-offs without cleats.

According to M. G. Bekker in Off-The-Road Locomotion, the shearing force can be augmented by the addition of cleats to the foot pads. The shearing force formula becomes

$$H = W \frac{h+s \tan \varphi}{s-h \tan \varphi} + \frac{bc(h^2+s^2)}{s-h \tan \varphi}$$

where b, s, and h are the cleat dimensions shown in Fig. 19a. Since the 1200 lb. lunar hopper will experience a peak acceleration of 5 g's on the lunar surface, which we assume will support 5 psi at a depth of 2 cm., a foot area of 1200 in^2 is necessary. With $h = s = 6$ in,

$$H = W\left[\frac{6+6(0.7)}{6-6(0.7)}\right] + \frac{6(.07)(36+36)}{6-6(0.7)}$$

$$H = W(5.67) + 16.8 \quad (LB)$$

*Apollo XI data now (7/23/69) upcoming may modify this conclusion.

The cohesive force is negligible. Since the cleat will be designed to operate in any direction, a T shape is required as shown in Fig. 19b. With this configuration, only half the weight on each cleat contributes to the production of shearing force in any one direction. This reduces H/W to 2.88. Cleat center-to-center spacing is found by another formula from Bekker to be

$$\ell_s = 1.8(s+h)$$

giving 21.6 in. between the foot segments for optimal operation. A more detailed analysis of the above material was presented in SUDAAR 359, semi-annual report, Ref. 5.

The lunar surface consists of 4 basic features: maria, craters, mountains, and rilles. The maria areas are mainly flat plains with rocky debris. Craters have diameters up to 200 kilometers while the mountains rise to 6 kilometers in height. The rilles are long trenches in the surface about 1 kilometer deep and a couple of kilometers wide. The terrain which the lunar hopper can traverse will depend to a large extent on the capabilities of the foot. It may be impossible for the pogo to hop across a rille, and the steepness of the slope which it can negotiate is still a matter of investigation.

A current study is being conducted at Jet Propulsion Laboratory (Space Program Summary 37-53 Vol. III, Oct. 31, 1968) to determine the effect of sloping soil surface on bearing capacity and shearing force. The soil being used is a cohesionless sand closely simulating the lunar soil. Most tests were made on wheels, but one test was conducted on a rectangular plate resting on a slope of 15°. The report states that there is "significant degradation of bearing capacity due to slope influences even at relatively low surface slopes compared to the soil angle of repose". It also points out the need for further investigation of soil thrust and slip on sloping terrain.

Another potential problem for hopping transport was brought to light by Surveyor VII. This craft landed near the rim of the crater Tycho in an area littered with rocky debris. Some of the rocks surrounding the craft were of a size (larger than 20 cm.) which might damage the foot

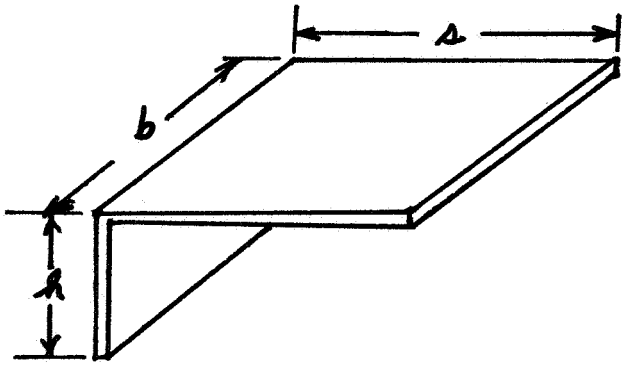

(a) Unidirectional

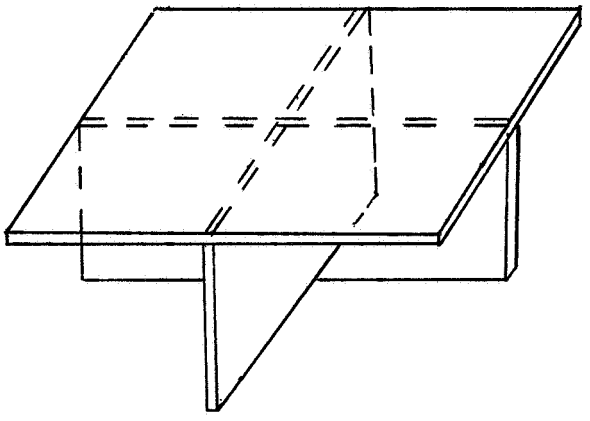

(b) Umnidirectional

Figure 19. Cleat Configuration.

structure of a hopper or make the area impassible. A table of rock size and frequency distribution, taken from the Surveyor VIII report, is given below.

ROCK WIDTH (CM)	NO. OF ROCKS PER 1000 M^2
80	1
20 to 80	67
15 to 20	106
10 to 15	347
5 to 10	5,100

It may be necessary to provide the foot segments with a type of suspension which enables the craft to land on smaller rocks while maintaining the majority of the foot segments in contact with the surface. Large pieces, say 80 cm. or more in size, could be avoided by the pilot. Spare foot segments would be carried on board in case of an emergency where a segment has been destroyed.

It becomes apparent that tests must be conducted on a lunar-type soil to obtain more information on the soil-foot interaction. A testing device has been proposed which would allow experiments concerning energy losses on landing and take-off, the omnidirectionality of cleat designs, shear resistance at different angles of take-off, and the degradation of performance on sloped surfaces. The Soil Impact Simulator consists of a variable angle slide containing a weight to which the foot segment is attached through an adjustable spring (Fig. 20). Withe the knowledge of height of the weight and the compression of the spring, energy losses can be calculated. Also the speed and force of impact can be varied to simulate the data from the lunar hopping transporter.

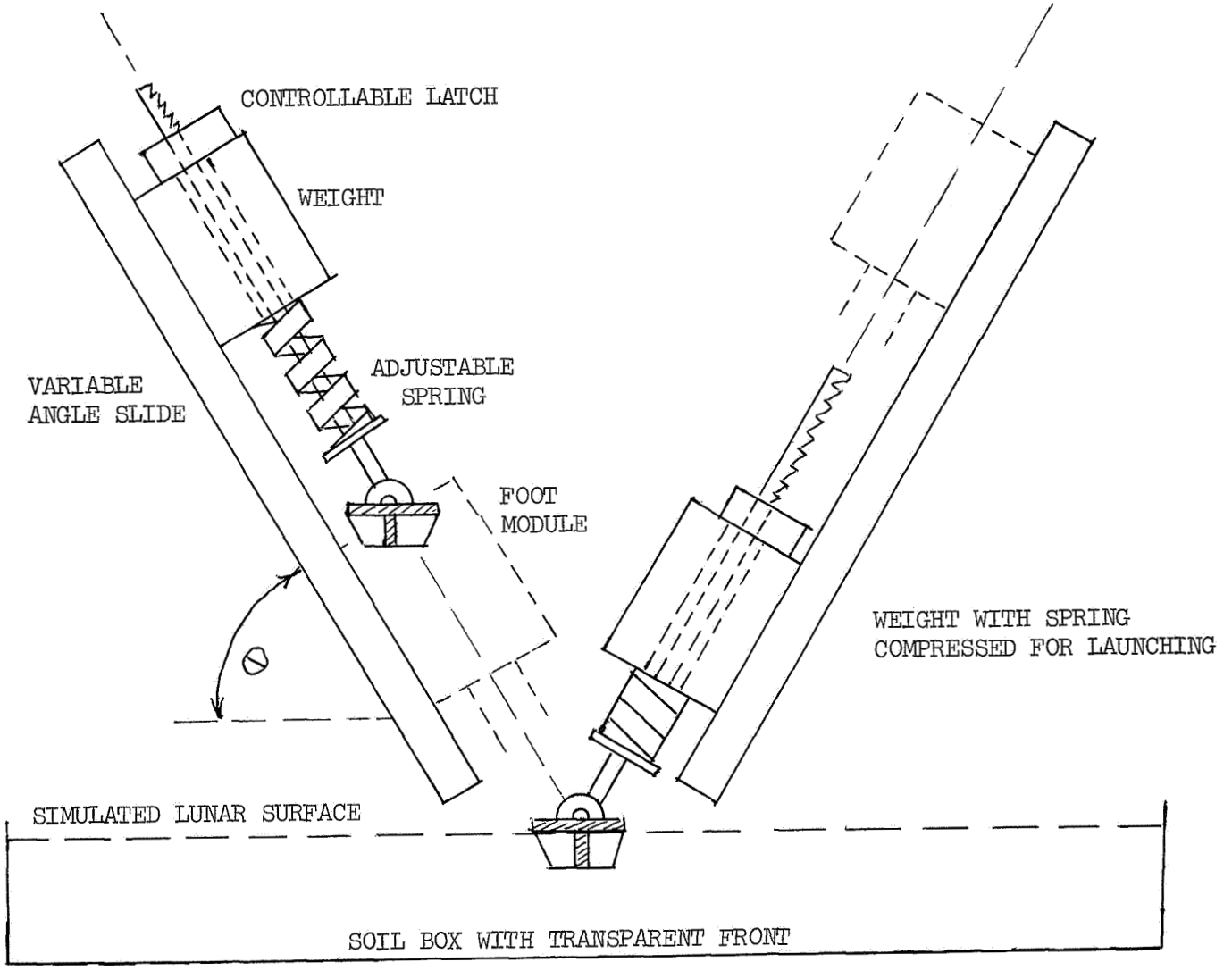

Figure 20. Soil Impact Simulator.

IX CONCLUSION

Substantial progress has been made over the last year in three areas of fundamental importance to the attainment of a hopping transport system; namely, procuring equipment for measurement of human acceleration tolerance, analysis of vehicle propulsion and stabilization performance, and fabrication of a terrestrial demonstrator vehicle.

Three other areas in which only a start has been made are: overall design, soil interaction, and detail guidance and control circuitry.

It is expected that data on human acceleration tolerance will be secured in the near future and that this will be followed at a later date by laboratory "flight" tests of a sub-scale twin-gyro programmable attitude-control system, and by landing and launch propulsion tests in simulated lunar soil.

The status of lunar hopping transportation vis-a-vis the rover and flyer concepts which are now being implemented by NASA will become much clearer in the next 12 to 18 months. So far, there is every indication that hopping is competitive with wheels or reaction jets, and in view of the obvious need for lunar mobility, continuation of the present program would appear to be a wise stratagem.

REFERENCES

1. Kaplan, M. H. and Seifert, H. S., "Investigation of a Hopping Transporter Concept for Lunar Exploration", Stanford University Department of Aeronautics and Astronautics, SUDAAR No. 348, (June 1968).

2. Seifert, H. S., "The Lunar Pogo Stick", Journal of Spacecraft and Rockets", Volume 4, No. 7, (July 1967).

3. Fraser, T. M., "Human Response to Sustained Acceleration", NASA SP-103, p. 1-9, (1966).

4. "Ballistic Missile and Space Vehicle Systems", H. Seifert and K. Brown, editors, John Wiley, 1961. See especially Chapter 20, "Integrated Design Analysis" by Millard Barton.

5. "Small Scale Lunar Surface Personnel Transporter Employing the Hopping Mode", Stanford University Department of Aeronautics and Astronautics, SUDAAR No. 359 (September 1968). Semi-Annual Report of NGR-05-020-258.

APPENDIX A

EQUATIONS FOR THE INITIAL AND FINAL PRESSURES THAT MUST BE ACHIEVED IN THE CYLINDER

To determine the initial pressure needed in the cylinder to attain a specified horizontal range and climb for a given set of piston displacements and to estimate the final pressure that must be reached in the cylinder to have an acceptable landing, a first-order model of the Lunar Pogo was set up.

A schematic of the first-order model in ballistic flight is shown in Fig. 21. The six basic time intervals in the operational sequence are:

$t_f \rightarrow t_o$: on ground

$t_o \rightarrow t_{e-}$: acceleration

$t_{e-} \rightarrow t_{e+}$: engagement (leg pickup)

$t_{e+} \rightarrow t_{d-}$: free flight

$t_{d-} \rightarrow t_{d+}$: disengagement (leg touchdown)

$t_{d+} \rightarrow t_f$: deceleration

Figure 22 is a schematic of the first-order model during acceleration. It shows the forces acting on the Lunar Pogo that determine the motion during acceleration. The motion during deceleration is quite similar to the motion during acceleration.

The following assumptions are made for the operational sequence:

1) There is no angular motion during acceleration or deceleration (one-dimensional motion).
2) The foot does not slide during acceleration or deceleration or adhere to the Lunar surface at engagement.
3) Engagement and disengagement are instantaneous.
4) The linear momentum of the system is conserved at engagement.
5) The foot loses all its momentum to the ground at disengagement, without affecting the main body.
6) The positional differences between the centers of mass of the system and of the main body alone are negligible for free flight.

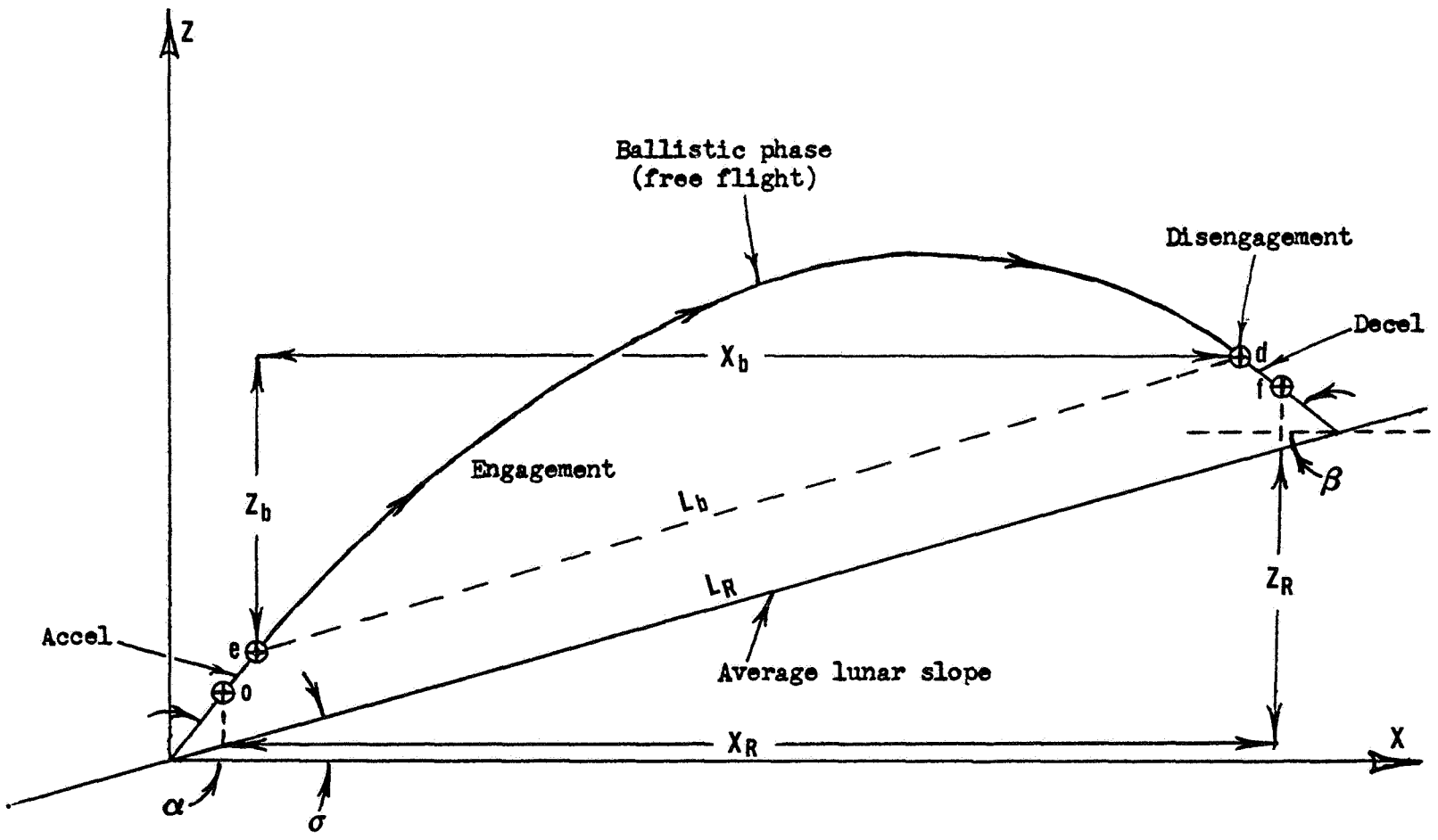

⊕ = center of mass (of main body)

Figure 21. First-Order Trajectory.

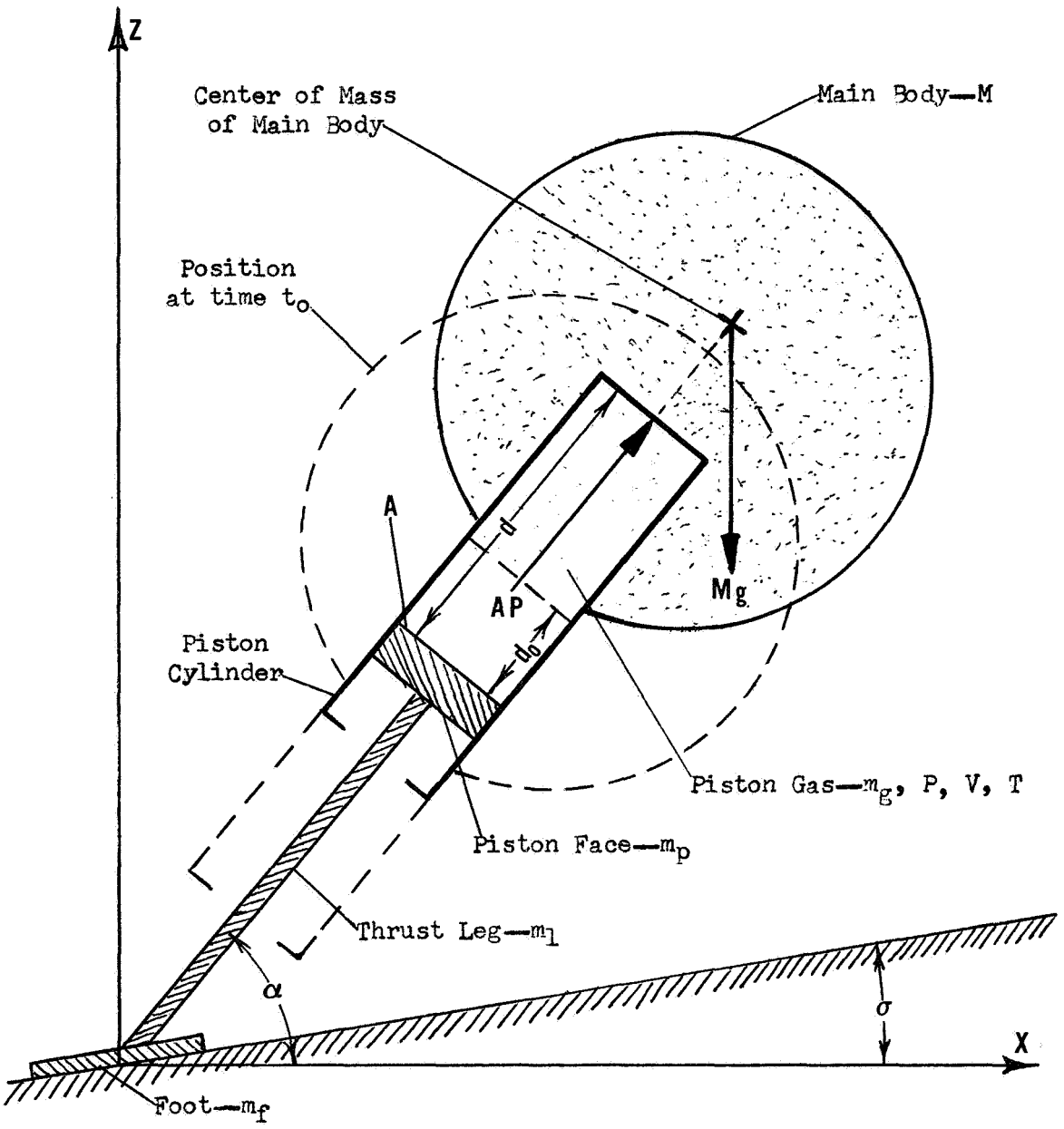

Figure 22. Acceleration Segment of First-Order Trajectory.

7) The average-slope rise line L_R is parallel to the ballistic rise line L_b, as shown in Fig. 21. That is, $\tan \sigma = (Z_R/X_R) \approx (Z_b/X_b)$.

8) The cylinder gas is a perfect gas $(PV = m_g RT)$ with constant specific heats $(E = m_g c_v T)$.

9) Adiabatic isentropic expansion during acceleration and compression during deceleration occur $(PV^\gamma = \text{const})$.

10) The gas composition is constant $(\gamma = \text{const})$.

11) The mass of the gas in the cylinder is negligible compared to the main body mass.

12) The equilibrium gas relations are valid for the dynamic situation.

13) Frictional forces between the piston and cylinder walls are negligible.

14) Launch is at optimum launch angle $\alpha_{opt} = \frac{\pi}{4} + \frac{\sigma}{2}$ (and, $\alpha_{opt} + \beta_{opt} = \frac{\pi}{2}$).

Under the preceding assumptions, the only forces that act in the axial direction on the main body during acceleration and deceleration are the pressure force and the axial component of the gravitational force. The relationship between pressure and piston cylinder displacement is:

$$Pd^\gamma = \text{const}$$

since $PV^\gamma = \text{const}$ and $V = Ad$, where A is constant for the cylinder. Then, summation of forces in the axial direction gives the following equation of motion of the main body during acceleration:

$$M \frac{d^2d}{dt^2} + Mg \sin \alpha = AP = AP_o(\frac{d_o}{d})^\gamma$$

For deceleration the corresponding equation of motion is:

$$M \frac{d^2d}{dt^2} + Mg \sin \beta = AP = AP_f(\frac{d_f}{d})^\gamma$$

These two equations can be analytically integrated to give the initial and final gas pressures in terms of the piston displacements and the main body velocities just before engagement and at disengagement. The integrated equations can be arranged in the following form:

$$P_o = \frac{Mg(\gamma-1)}{A} \frac{[\frac{v_{e-}^2}{2gd_o} + (\frac{d_e}{d_o} - 1)\sin\alpha]}{[1-(\frac{d_o}{d_e})^{(\gamma-1)}]}$$

$$P_f = \frac{Mg(\gamma-1)}{A} \frac{[\frac{v_{d+}^2}{2gd_f} + (\frac{d_d}{d_f} - 1)\sin\beta]}{[1-(\frac{d_f}{d_d})^{(\gamma-1)}]}$$

During free flight the only external force acting on the system is gravity. Then, the equations of motion for the system center of mass are:

$$\frac{d^2X}{dt^2} = 0$$

$$\frac{d^2Z}{dt^2} = -g$$

Integrating and applying the appropriate boundary conditions to the free flight equations of motion gives:

$$X_b = v_{e+}t_b \cos\alpha$$

$$Z_b = v_{e+}t_b \sin\alpha - \frac{1}{2} gt_b^2$$

Noting that $\tan\sigma = (Z_R/X_R) \approx (Z_b/X_b)$, Z_b and t_b are eliminated from the preceding two equations to give:

$$X_b = \frac{2v_{e+}^2}{g} \cos^2\alpha(\tan\alpha - \tan\sigma)$$

Kinetic plus potential energy is conserved during free flight, so that:

$$\frac{1}{2} v_{e+}^2 = \frac{1}{2} v_{d+}^2 + gX_b \tan\sigma$$

From the geometry of Fig. 21:

$$X_R = X_b + (d_e-d_o)\cos\alpha + (d_d-d_f)\cos\beta$$

Since momentum is conserved at enegagement:

$$v_{e-} = (1 + \frac{m}{M})v_{e+}$$

while at disengagement:

$$v_{d+} = v_{d-}$$

Now, assuming launch is at optimum launch angle $\alpha = \alpha_{opt}$, the five preceding equations are combined with the equations for P_o and P_f to give:

$$P_o = \frac{Mg(\gamma-1)}{2A}\left\{(1 + \frac{m}{M})^2\left[\frac{X_R}{d_o} - (\frac{d_e}{d_o} - 1)\cos\alpha_{opt} - (\frac{d_d}{d_o} - \frac{d_f}{d_o})\sin\alpha_{opt}\right]\cdot \tan\alpha_{opt} + 2(\frac{d_e}{d_o} - 1)\sin\alpha_{opt}\right\} \Bigg/ \left[1-(\frac{d_o}{d_e})^{(\gamma-1)}\right]$$

$$P_f = \frac{Mg(\gamma-1)}{2A} \frac{\left\{\frac{X_R}{d_f}\cot\alpha_{opt} + [(\frac{d_d}{d_f} - 1) - (\frac{d_e}{d_f} - \frac{d_o}{d_f})\cot\alpha_{opt}]\cos\alpha_{opt}\right\}}{\left[1-(\frac{d_f}{d_d})^{(\gamma-1)}\right]}$$

For $40^\circ < \alpha_{opt} < 50^\circ$, the terms involving the ratios of the displacements will normally be very small compared to either X_R/d_o or X_R/d_f, and will partially cancel. Also, for expected values of m/M, $(1 + m/M)^2 \approx (1 + 2\frac{m}{M})$. Then, with a maximum error of less than 1%, the equations for P_o and P_f can be simplified to:

$$P_o = \frac{(M+2m)g(\gamma-1)}{2A\left[1-(\frac{d_e}{d_o})^{(\gamma-1)}\right]}(\frac{X_R}{d_o})\tan\alpha_{opt} \qquad (1a)$$

$$P_f = \frac{Mg(\gamma-1)}{2A\left[1-(\frac{d_f}{d_d})^{(\gamma-1)}\right]}(\frac{X_R}{d_f})\cot\alpha_{opt} \qquad (2a)$$

APPENDIX B

TEMPERATURE-PRESSURE-MASS RELATIONSHIPS FOR GAS TRANSFER BETWEEN GAS RESERVOIRS

The relationships between the equilibrium gas temperatures, equilibrium gas pressures, and masses of gas are derived for the transfer of gas through a pressure differential from one reservoir to a second one at a lower pressure.

Consider the system shown in Fig. 23. The subscripts "A" and "B" indicate Reservoirs "A" and "B" respectively. For the flow as indicated in Fig. 23, pressure P_A is always greater than pressure P_B. At time $t = t_1$ — corresponding to state "1", the valve begins to open so that gas flows from Reservoir "A" to Reservoir "B". The valve is closed before the pressures equalize. At a later time $t = t_2$ — corresponding to state "2", the valve is completely closed.

In addition to the assumptions listed in Appendix A with regard to the gas, the following assumptions are made for the gas flow:

1) There is no heat flow between the reservoirs or through the reservoir walls.
2) Frictional losses at the valve and at the reservoir walls are neglected.
3) Body forces acting on the gas are negligible.
4) States "1" and "2" are equilibrium states.
5) The total temperature of the gas in either reservoir is constant throughout the reservoir at any time (no gradients).

Control volumes are drawn about Reservoirs "A" and "B" as shown in Fig. 24. Consider an arbitrary control volume V_{ol} enclosed by a surface S_{ur}. Under the assumptions made, the general energy equation at constant volume reduces to:

$$\frac{d}{dt}\int_{V_{ol}} (e + \frac{1}{2} v_g^2)\rho d\tau = -\oint_{S_{ur}} (e + \frac{1}{2} v_g^2 + \frac{P}{\rho})\rho \bar{v}_g \cdot \hat{n} dS$$

and the continuity equation is:

$$\frac{d}{dt}\int_{V_{ol}} \rho d\tau = -\oint_{S_{ur}} \rho \bar{v}_g \cdot \hat{n} dS$$

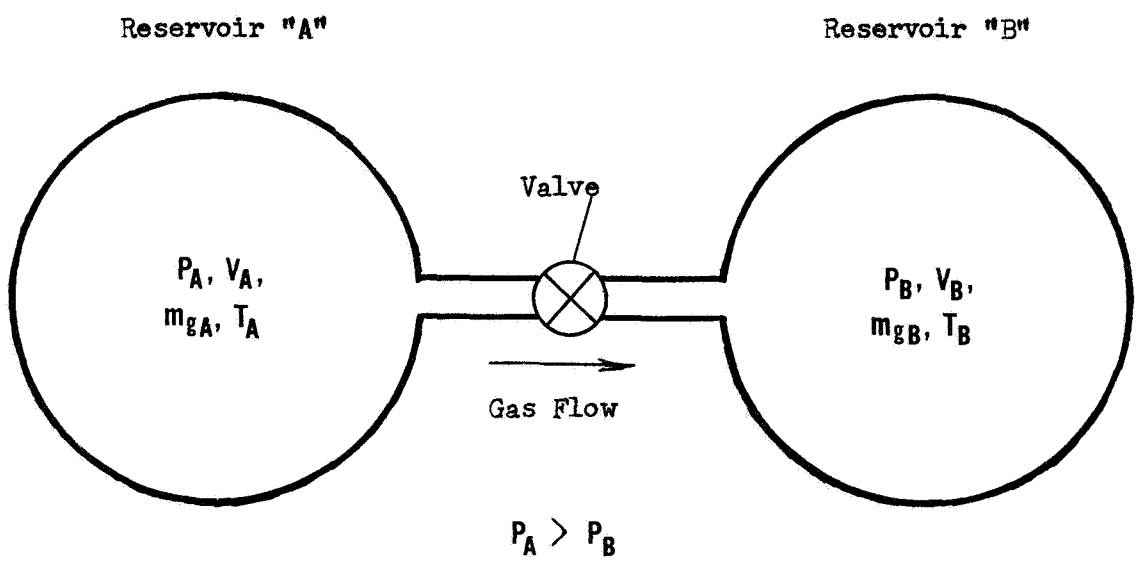

Figure 23. Gas Flow Between Two Reservoirs.

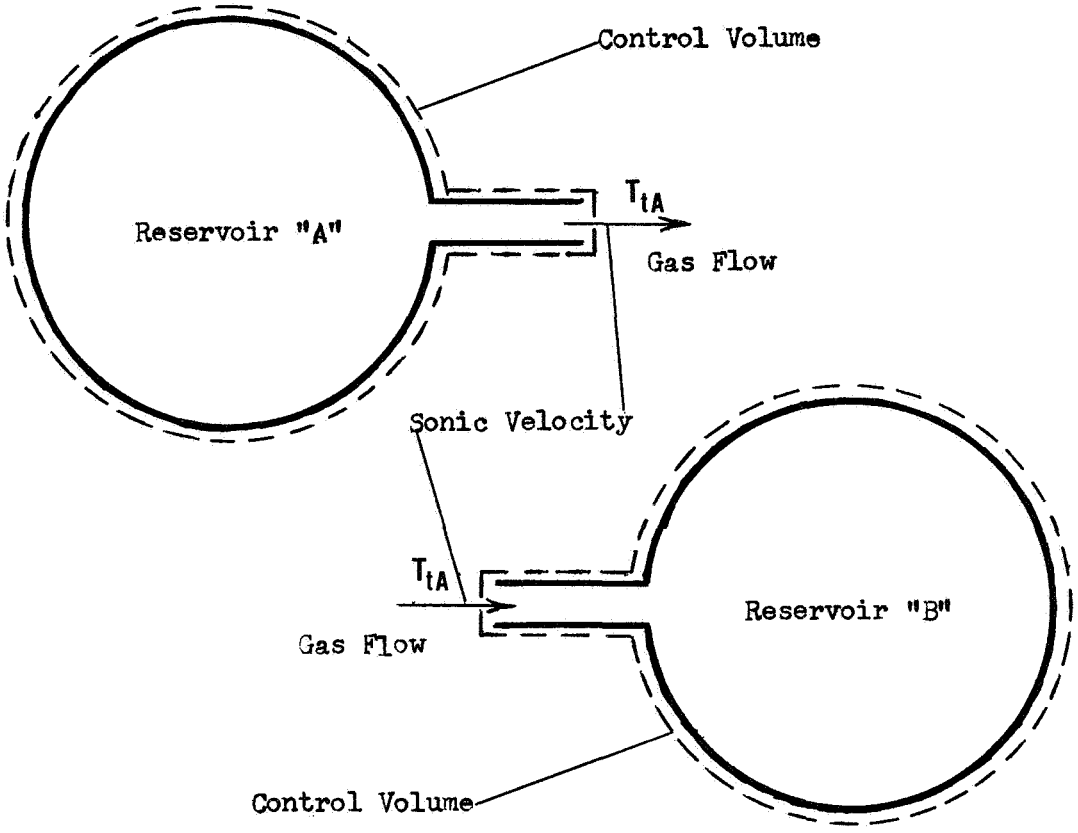

Figure 24. Control Volumes for Gas Flow Between Two Reservoirs.

Since the gas is completely perfect:

$$e + \frac{1}{2} v_g^2 + \frac{P}{\rho} = h + \frac{1}{2} v_g^2 = h_t = c_p T_t$$

Then, the right hand side of the energy equation becomes:

$$-\oint_{S_{ur}} (e + \frac{1}{2} v_g^2 + \frac{P}{\rho}) \rho \bar{v}_g \cdot \hat{n} dS = -\oint_{S_{ur}} c_p T_t \rho \bar{v}_g \cdot \hat{n} dS$$

$$= -\oint_{S_{ur}} (c_p T_t)_{\substack{\text{mass} \\ \text{flux}}} \rho \bar{v}_g \cdot n dS = -(c_p T_t)_{\substack{\text{mass} \\ \text{flux}}} \oint_{S_{ur}} \rho \bar{v}_g \cdot \hat{n} dS$$

$$= (c_p T_t)_{\substack{\text{mass} \\ \text{flux}}} \frac{d}{dt} \int_{V_{ol}} \rho d\tau = c_p (T_t)_{\substack{\text{mass} \\ \text{flux}}} \frac{dm_g}{dt}$$

where $c_p T_t = (c_p T_t)_{\text{mass flux}}$ since $\rho \bar{v} \cdot \hat{n} dS$ is the mass flux through the boundary S_{ur}, $(T_t)_{\text{mass flux}}$ is assumed constant, and $m_g = \int_{V_{ol}} \rho d\tau$ is the mass of gas enclosed by S_{ur}.

Next, the relations:

$$c_p T_t = h_t = h + \frac{1}{2} v_g^2 = c_p T + \frac{1}{2} v_g^2$$

$$c_p - c_v = R$$

$$\frac{c_p}{c_v} = \gamma$$

can be combined to give

$$e + \frac{1}{2} v_g^2 = c_v T_t (1+\epsilon)$$

where

$$\epsilon = \frac{(\gamma-1)^2}{2} \left(\frac{T}{T_t}\right) \frac{v_g^2}{\gamma R T}$$

The integral of $e + \frac{1}{2} v_g^2$ over the mass enclosed by S_{ur} becomes:

$$\int_{V_{ol}} (e + \tfrac{1}{2} v_g^2)\rho d\tau = \int_{V_{ol}} (1 + \epsilon)c_v T_t \rho d\tau$$

$$= c_v T_t \int_{V_{ol}} (1 + \epsilon)\rho d\tau$$

For the actual flow problem being considered, the maximum gas velocity occurs at the valve. If this velocity is sonic, then $(T/T_t) = 2/(\gamma+1)$ and $v_g^2 = \gamma RT$, so that:

$$\epsilon_{max} = \frac{(\gamma-1)^2}{2}\left(\frac{2}{\gamma+1}\right) = \frac{(\gamma-1)^2}{(\gamma+1)}$$

$$= \frac{1}{15}$$

for a gas with $\gamma = 1.4$. Elsewhere in either of the reservoirs, the gas velocity is much smaller. Then, if V_{ol} corresponds to the control volume about either Reservoir "A" or "B", ϵ may be neglected compared to unity, so that:

$$\int_{V_{ol}} (e + \tfrac{1}{2} v_g^2)\rho d\tau = c_v T_t \int_{V_{ol}} \rho d\tau$$

$$= c_v T_t m_g$$

The energy equation for either of the control volumes becomes:

$$\frac{d}{dt}(c_v T_t m_g) = c_p (T_t)_{\substack{\text{mass} \\ \text{flux}}} \frac{dm_g}{dt}$$

or

$$\frac{d}{dt}(m_g T_t) = \gamma (T_t)_{\substack{\text{mass} \\ \text{flux}}} \frac{dm_g}{dt}$$

For this flow problem, the mass flux is from Reservoir "A" to Reservoir "B", so that $(T_t)_{\text{mass flux}} = T_{tA}$ always. Applying the energy equation to Reservoirs "A" and "B" then yields:

$$\frac{d}{dt}(m_{gA}T_{tA}) = \gamma T_{tA}\frac{dm_{gA}}{dt} \tag{1b}$$

$$\frac{d}{dt}(m_{gB}T_{tB}) = \gamma T_{tA}\frac{dm_{gB}}{dt} \tag{2b}$$

The total mass of gas in the two reservoirs $m_{gA} + m_{gB} = m_{gA1} + m_{gB1}$ is constant, so:

$$\frac{dm_{gA}}{dt} + \frac{dm_{gB}}{dt} = 0 \tag{3b}$$

Equations (1b), (2b), and (3b) can now be integrated and combined with the equation of state $(PV = m_gRT)$ for the reservoirs to determine the new gas temperature and the new masses of gas in the reservoirs in terms of the new pressures, the old temperatures, pressures, and masses, and other constants. For a general case with two finite reservoirs of volumes V_A and V_B, the new temperature T_{B2} and new mass of gas m_{gB2} in Reservoir B, the reservoir being filled are:

$$\frac{T_{B2}}{T_{B1}} = \frac{\dfrac{P_{B2}}{P_{B1}}}{1 + \dfrac{P_{A1}}{P_{B1}}\dfrac{T_{B1}}{T_{A1}}\dfrac{V_A}{V_B}\left\{1 - \left[1 - \dfrac{P_{B1}}{P_{A1}}\dfrac{V_B}{V_A}\left(\dfrac{P_{B2}}{P_{B1}} - 1\right)\right]^{1/\gamma}\right\}} \tag{4b}$$

$$\frac{m_{gB2}}{m_{gB1}} = 1 + \frac{P_{A1}}{P_{B1}}\frac{T_{B1}}{T_A}\frac{V_A}{V_B}\left\{1 - \left[1 - \frac{P_{B1}}{P_{A1}}\frac{V_B}{V_A}\left(\frac{P_{B2}}{P_{B1}} - 1\right)\right]^{1/\gamma}\right\} \tag{5b}$$

The equations for T_{A2} and m_{gA2} are similar. Since states "1" and "2" are equilibrium states, the total and static temperatures are equal. Consequently, the total temperatures have been replaced by the static temperatures in Equations (4b) and (5b).

There are two important cases of this gas transfer process. The first case is that in which gas is added to the low pressure reservoir from an infinite reservoir. Reservoir "A" becomes an infinite reservoir. Then, $P_{A2} = P_{A1} = P_A$, $T_{A2} = T_{A1} = T_A$, and $V_A \to \infty$. Equations (4b) and (5b)

reduce to:

$$\frac{T_{B2}}{T_{B1}} = \frac{\gamma}{\frac{P_{B1}}{P_{B2}}\left(\gamma - \frac{T_{B1}}{T_A}\right) + \frac{T_{B1}}{T_A}} \tag{6b}$$

$$\frac{m_{gB2}}{m_{gB1}} = 1 + \frac{1}{\gamma}\frac{T_{B1}}{T_A}\left(\frac{P_{B2}}{P_{B1}} - 1\right) \tag{7b}$$

The second case is that in which gas is vented from one reservoir into an infinite low pressure reservoir (or vacuum). Then, $P_{B2} = P_{B1} = P_B$, $T_{B2} = T_{B1} = T_B$, and $V_B \to \infty$. For this case, only Equation (1b) is needed. It is easily integrated to give:

$$\frac{T_{A2}}{T_{A1}} = \left(\frac{P_{A2}}{P_{A1}}\right)^{\left(\frac{\gamma-1}{\gamma}\right)} \tag{8b}$$

$$\frac{m_{gA2}}{m_{gA1}} = \left(\frac{P_{A2}}{P_{A1}}\right)^{\frac{1}{\gamma}} \tag{9b}$$

Equations (4b)-(9b) can now be used to examine the process of gas transfer from one reservoir to another.

APPENDIX C

COMPUTER MODEL OF LUNAR POGO PROPULSION DYNAMIC OPERATING CYCLE

In order to estimate the amount of propulsion gas needed for the Lunar Pogo, a dynamic model of the operating cycle for a sequence of hops has been set up. This model covers all phases of hopping: on ground, acceleration, free flight, and deceleration. Although the model is quite simplified, it gives a good qualitative idea of the interactions in the hopping process and quantitative estimate of the mass of gas needed.

All pressure changes in the cylinder are made by adding or venting gas. Gas is added to the cylinder from a gas accumulator and is vented from the cylinder to the vacuum of the moon. Pressure changes must be made at two times for a hop. While the Pogo is on the ground and a horizontal range and climb have been selected, the pressure is adjusted to attain this range and climb. During free flight (or, equivalently, at the beginning of deceleration), the pressure is adjusted to attain a proper landing, i.e., terminal piston position.

For the model, all the assumptions of Appendices A and B are made, in addition to the following assumptions:

1) For a hop $d_d = d_e$, that is, the piston displacement is not changed during free flight.
2) The launch is at optimum launch angle α_{opt}.
3) The pressure and temperature of the gas in the accumulator supplying the cylinder are constant during the times of gas addition.

Under all of these assumptions and with appropriate symbol changes, Equations (6b)-(9b) are then used to describe the gas temperature and mass changes for adding and venting of gas during a hop. Equations (1a) and (2a) are used to determine the initial gas pressure needed for a hop and the final gas pressure that must be attained. The adiabatic expansion relations (from $PV^{\gamma} = \text{const}$):

$$Pd^{\gamma} = \text{const} \tag{1c}$$

$$Td^{(\gamma-1)} = \text{const} \tag{2c}$$

are used to determine the pressure and temperature changes during acceleration and deceleration. With these sets of equations, the complete pressure, temperature, mass transfer, and piston displacement cycle can be followed through a hop. Figure 25 shows how these equations are arranged to follow P, T, m_g, and d through a hop.

A sequence of hops is now formed by specifying: (1) a set of ranges and launch angles, (2) a set of piston displacements for each hop, (3) the initial conditions of the gas before the first hop, (4) the temperature variation of the gas in the accumulator from hop to hop, and (5) the variation in main body mass from hop to hop. The flow chart in Figure 25 is then used to follow the gas pressure, temperature, and mass through the sequence of hops.

To see how the flow chart works, assume (n-1) hops of a sequence have been completed, and the Pogo is on the ground about to begin hop n. P_f, T_f, and m_{gf} for hop (n-1) are known. For hop n the parameters d_o, $d_e = d_d$, d_f, M, T_{acc}, X_R, and α_{opt} are specified. P_o for hop n (that must be used to achieve the specified range and climb) is calculated. If P_o for hop n is greater than P_f for hop (n-1), gas must be added to the cylinder while the Pogo is on the ground. Otherwise, gas is vented. T_o and m_{go} for hop n are now calculated from the appropriate relationships. The Pogo goes through acceleration and P_e and T_e are determined.

The Pogo enters free flight. P_f for hop n (that must be reached to achieve the specified d_d and d_f) is calculated. From P_f a step back is taken to calculate P_d. If P_e is greater than P_d, gas is vented from the cylinder while the Pogo is in flight. Otherwise, gas is added. T_d and m_{gd} are calculated from the appropriate relationships. The Pogo goes throught deceleration and T_f is determined. This completes hop n. P_f, T_f, and m_{gf} are known at the end of hop n. Hop (n+1) can then be started by specifying d_o, $d_e = d_d$, d_f, M, T_{acc}, X_R, and α_{opt} for it.

The flow chart of Fig. 25 was written into a computer program. Several sequences of hops were then considered. For all of these sequences, the following additional assumptions were made:

1) d_o, $d_e = d_d$, d_f, M, and T_{acc} are the same for all hops.

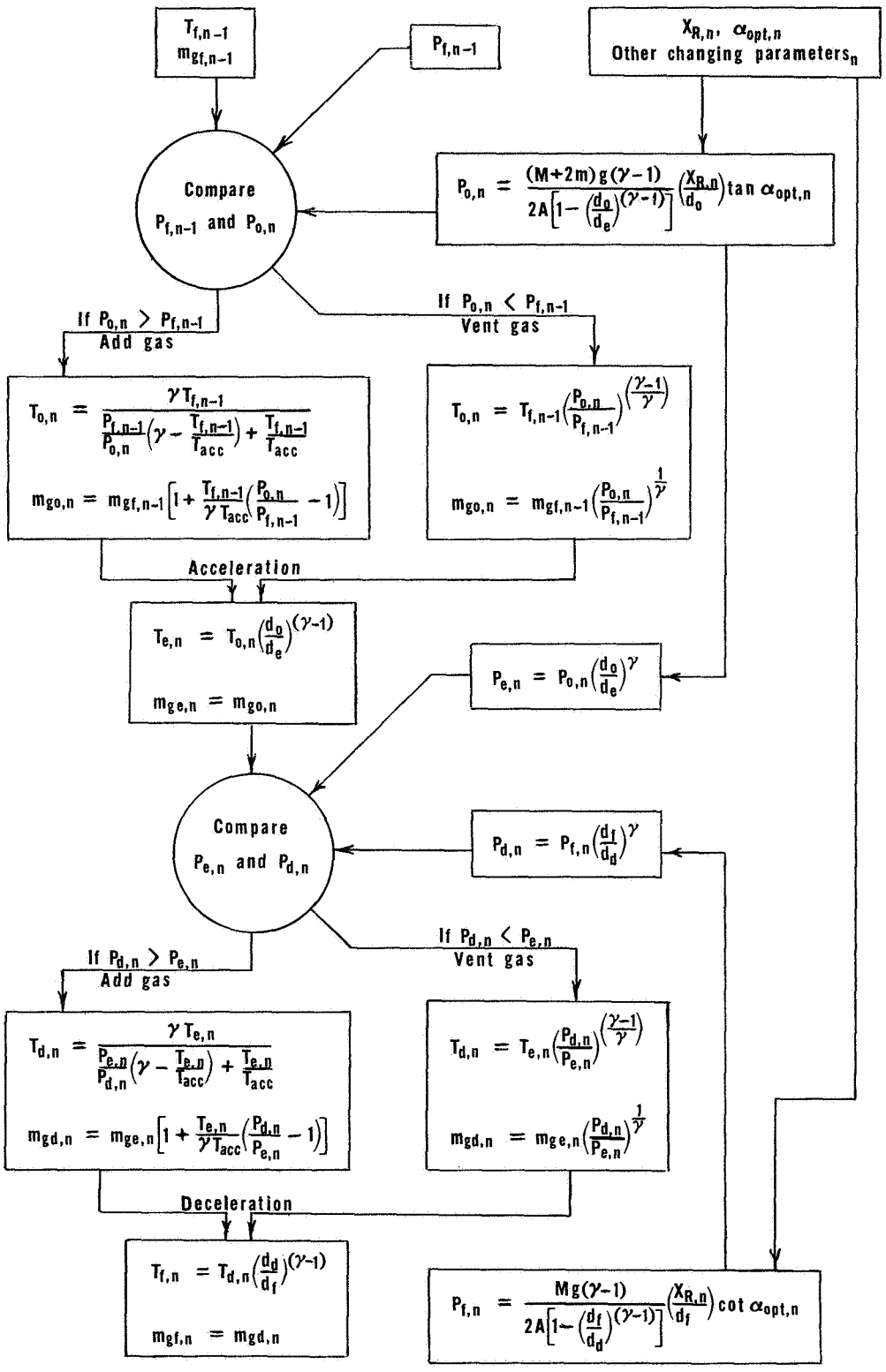

Figure 25. Flow Chart for Hopping Cycle Parameters

2) $d_f = d_o$ for all hops.

3) The cylinder is empty before the first hop.

Most of the hopping sequences examined were carried out to about 40 hops - far enough to see what the long term gas state effects in the cylinder were.

Among the sequences examined was one in which the lunar terrain consisted of a 50 ft level grade, a 50 ft uphill slope at $\sigma = 10^o$, and a 50 ft downhill slope at $\sigma = -10^o$ - the pattern being continuously repeated. The Pogo parameters used for this sequence were:

$M = 38$ slug $\qquad T_{acc} = 530^oR$

$m = 2$ slug $\qquad A = 28.3$ in^2

$\gamma = \gamma(N_2) = 1.40$ $\qquad d_f = d_o = 1$ ft

$R = R(N_2) = 1775$ ft-lb/slug-^oR $\qquad d_d = d_e = 3$ ft

$g = 5.31$ ft/sec^2

Figure 12 shows the Pogo doing a set of three hops over the lunar terrain at the beginning of this sequence (dotted lines). Another set of three identical hops at a later point in this sequence is also shown.

Note, that for identical hops (range and launch angle), the gas temperatures are lower and the gas masses are higher for the later hops than for the earlier ones. The "average" specific energy (energy per unit mass) of the gas is lower for the later hops. If a third set of hops at a still later point were also known, the gas temperature would be lower and the gas masses would be higher than for the first two sets, but only very slightly different from the second set of hops. Thus, for this model - at least, there is a secular change in the condition of the cylinder gas. For a sequence of hops, which "on the average" is over level terrain, the average specific energy of the cylinder gas decreases from its value for the initial hops of a sequence to a value which is nearly constant for hops at a point sufficiently late in the sequence.

Using the hopping sequence described, an estimate of the amount of gas needed for a mission of 1000 hops was made. From the increments of gas added to the cylinder for each hop, the mean amount of gas added per hop was determined. Summation of this mean amount of gas for 1000

hops and addition of a gas allowance of 75% to cover initial filling of the cylinder, refillings if necessary, rougher terrains (slopes steeper than $\sigma = \pm 10^{o}$), launches at non-optimum angles, ullage, and a safety reserve then led to the total amount of gas estimated for the Pogo as stated on pp. 40-45 of Ref. 5 (SUDAAR 359, Semi-Annual Report).

APPENDIX D

OPTIMUM PISTON DISPLACEMENT RATIO

There is an optimum piston expansion ratio $(d_e/d_o)_{opt}$. Operating at $(d_e/d_o) = (d_e/d_o)_{opt}$ minimizes the initial pressure and consequently the initial acceleration. From Appendix A, the equation for P_o is:

$$P_o = \frac{(M+2m)g(\gamma-1)}{2A[1-(d_o/d_e)^{(\gamma-1)}} (X_R/d_o) \tan \alpha_{opt}$$

For a constant d_e, the optimum d_o and consequently $(d_e/d_o)_{opt}$ is found by setting $(\partial P_o/\partial d_o) = 0$. Then:

$$\frac{\partial P_o}{\partial d_o} = \frac{\partial}{\partial d_o} \left\{ \frac{(M+2m)g(\gamma-1)}{2A[1-(d_o/d_e)^{(\gamma-1)}]}(X_R/d_o) \tan \alpha_{opt} \right\}$$

$$= \frac{(M+2m)g(\gamma-1)X_R \tan \alpha_{opt}}{2Ad_o^2[1-(d_o/d_e)^{(\gamma-1)}]^2} [\gamma(d_o/d_e)^{(\gamma-1)}-1]$$

$$= 0$$

or:

$$\gamma(d_o/d_e)^{(\gamma-1)}-1 = 0$$

Solving for (d_o/d_e) gives:

$$(d_e/d_o)_{opt} = \gamma^{(\frac{1}{\gamma-1})} \tag{1d}$$

Similarly, operating at $(d_d/d_f) = (d_d/d_f)_{opt} = \gamma^{(\frac{1}{\gamma-1})}$ will minimize the final pressure and the final acceleration.

APPENDIX E

PROPULSION ANALYSIS SYMBOL DEFINITIONS

A	area of piston face
E	internal energy
L_b	ballistic rise line
L_R	average-slope rise line
M	main body mass
P	gas pressure
R	gas constant
S	surface
T	gas temperature
V	volume
X	horizontal coordinate
X_b	ballistic range
X_R	horizontal range
Z	vertical coordinate
Z_b	ballistic climb
Z_R	vertical climb
a	acceleration
c_p	specific heat at constant pressure
c_v	specific heat at constant volume
d	displacement of piston cylinder
e	specific internal energy
g	acceleration of lunar gravity
g_o	acceleration of terrestial gravity
h	specific enthalpy

k_{eff}	effective force constant
m	$m_f + m_l + m_p$
m_f	mass of foot
m_g	mass of gas
m_l	mass of thrust leg
m_p	mass of piston face
$\dot{m}_{gmax}$	maximum mass flow rate through valve
Δm_g	mass of gas added per hop
n	number of hop
$\hat{n}$	unit outward normal
t	time
v	velocity of center of mass of main body or system
v_g	gas velocity
α	launch angle
β	landing angle
γ	specific heat ratio
ϵ	$\frac{(\gamma-1)^2}{2}(\frac{T}{T_t})\frac{v_g^2}{\gamma RT}$
ρ	mass density of gas

SUBSCRIPTS

A	Reservoir "A"
B	Reservoir "B"
acc	accumulator
atm	atmospheric (terrestrial)
d	disengagement
e	engagement

f	final
max	maximum
o	initial
opt	optimum
p	pickup (of leg)
t	total
1	state "1"
2	state "2"
+	plus
-	minus

APPENDIX F

ANGULAR OFFSET ϵ REQUIRED TO PROVIDE $\dot{\theta} = 0$ AT $\theta = 0$ UPON LANDING

When the vehicle lands, the main body moves down the leg compressing the gas in the cylinder. So the mass center to pivot point distance is not constant. Assume that the foot and leg lose their kinetic energy instantaneously upon impact. Referring to the coordinate of Fig. 13, the equations of motion assuming no foot slippage and a free pivot are

$$m\ddot{r} - mr\dot{\theta}^2 + mg \cos \theta = AP_o\left(\frac{d_o}{r-r_o+d_o}\right)^{\gamma}$$

$$I_p\ddot{\theta} + 2mr\dot{r}\dot{\theta} - mgr \sin \theta = 0$$

The term $Ap_o[d_o/(r-r_o+d_o)^{\gamma}]$ is the force that the compressed gas exerts on the main body. The initial conditions for these differential equations at $t = t_d$ (disengagement) are

$$\theta(t_d) = \theta_d \qquad r(td) = rd$$

$$\dot{\theta}(t_d) = -\frac{v(t_d)}{r(t_d)} \sin \epsilon \qquad \dot{r}(t_d) = -v(t_d) \cos \epsilon$$

An iterative procedure must be used to determine the value of epsilon such that the vehicle will come to the vertical with zero angular velocity.

APPENDIX G

CALCULATION OF CONTROL MOMENTS FOR TYPICAL LUNAR HOP

Symbols relating to the hopper are defined in Appendix H and Figure 14. The governing linearized equations are

$$\begin{bmatrix} S^2 & \frac{2h}{I} S \\ -\frac{[(h+k_{\dot\theta})S+k_\theta]}{J} & S^2 + \frac{b}{J} S \end{bmatrix} \begin{bmatrix} \Theta \\ \Phi \end{bmatrix} = \begin{bmatrix} \frac{M_{ext}}{I} + S\theta(0) + \dot\theta(0) + \frac{2h}{I}\varphi(0) \\ -\frac{k_\theta}{J}\Theta_c + (S+\frac{b}{J})\dot\phi(0) - \frac{(h+k_{\dot\theta})}{J}\theta(0) + \dot\phi(0) \end{bmatrix}$$

The characteristic equation of this matrix is

$$S^4 + \frac{b}{J} S^3 + \frac{2h}{IJ}(h + k_{\dot\theta})S^2 + \frac{2hk_\theta}{IJ} S = 0$$

Assume $\varphi(0)$ and $\dot\phi(0)$ are both zero. Then,

$$\Theta = \frac{(S^2 + \frac{b}{J} S)[\frac{M_{ext}}{I} + S\theta(0) + \theta(0)] + \frac{2hk_\theta}{IJ} S\,\Theta_c + \frac{2h(h+k_{\dot\theta})}{IJ} S\theta(0)}{S[S^3 + \frac{b}{J} S^2 + \frac{2h}{IJ}(h + k_{\dot\theta})S + \frac{2hk_\theta}{IJ}}$$

$$\Phi = \frac{[\frac{(h+k_{\dot\theta})S + k_\theta}{J}][M_{ext} + S\theta(0) + \dot\theta(0)] - [\frac{k_\theta}{J}\Theta_c + (\frac{h+k_{\dot\theta}}{J})\theta(0)]S^2}{S[S^3 + \frac{b}{J} S^2 + \frac{2h}{IJ}(h+k_{\dot\theta})S + \frac{2hk_\theta}{IJ}]}$$

After lift-off, the vehicle must be rotated to the proper landing orientation. If we assume a 45° launch angle and no change in elevation, the landing angle is -45° or a net rotation of 90°. This will be the most critical requirement on the control system. The vehicle must accomplish this maneuver in about 4 seconds for a typical 50 ft. hop. For example, assume $\theta(0) = \dot\theta(0) = 0$, $M_{ext} = 0$, and $\theta_c = \pi/2$. Then the above equations become

$$\Theta = \frac{\frac{2hk_\theta}{IJ}(\pi/2)}{S(S^3 + \frac{b}{J} S^2 + \frac{2h}{IJ}(h+k_{\dot\theta})S + \frac{2hk_\theta}{IJ})}$$

$$\Phi = \frac{-\frac{k_\theta}{J}(\pi/2)}{s[S^3 + \frac{b}{J}S^2 + \frac{2h}{IJ}(h+k_{\dot\theta})S + \frac{2hk_\theta}{IJ}]}$$

A preliminary estimate is that the moment of inertia of the vehicle is $I = 400$ kg-m^2. Assume $h = 200$ kg-m^2/sec for each gyro wheel and let each have a radius of gyration of 0.25 meter. Choose $\omega = 300$ rad./sec., then $m = 10.6$ kg. Assuming the wheel to be a thin disk, $J = 0.333$ kg-m^2. The characteristic equation becomes

$$S^3 + 3.0\,bS^2 + 3.0(200 + k_{\dot\theta})S + 3.0\,k_\theta = 0$$

or

$$-3k_\theta = S[S^2 + 3bS + 3(200 + k_{\dot\theta})]$$

We are dealing with a third order system, and desire the response time (i.e., the time when θ reaches 95% of its steady state value) to be 4 seconds. Also, zero overshoot is desirable. Zero overshoot can be accomplished as long as the simple pole lies on or to the right of the line joining the complex poles. These requirements can be met with ω_n between 1 and 2 rad./sec. and $\alpha/\xi\omega_n$ between 0.7 and 1, where α is the location of the real pole.

The problem then becomes one of locating the open loop poles so that the root locus passes through an acceptable region of the complex plane. For example, choose open loop poles at $-1.8\pm1.6j$, 0. Then $b = 1.2$ and $k_{\dot\theta} = -198.1$. For these poles the root locus versus k_θ is shown in Fig. 26. The minimum of the locus meets the requirement for closed loop poles and corresponds to a gain $k_\theta = 0.953$ (the system goes unstable at a gain $k_\theta = 21$). At this gain, the roots of the characteristic equation are $s = -1.2\pm1.2j$, -1.0. Consequently,

$$\Theta(S) = \frac{4.49}{S[(S+1)(S+1.2+1.2j)(S+1.2-1.2j)} = \frac{4.49}{S(S+1)(S^2+2.4S+2.88)}$$

Expanding into parial fractions, there results

$$\theta(S) = \frac{1.57}{S} + \frac{-3.03}{S+1} + \frac{.738(1-0.715j)}{S+1.2+1.2j} + \frac{.738(1+0.715j)}{S+1.2-1.2j}$$

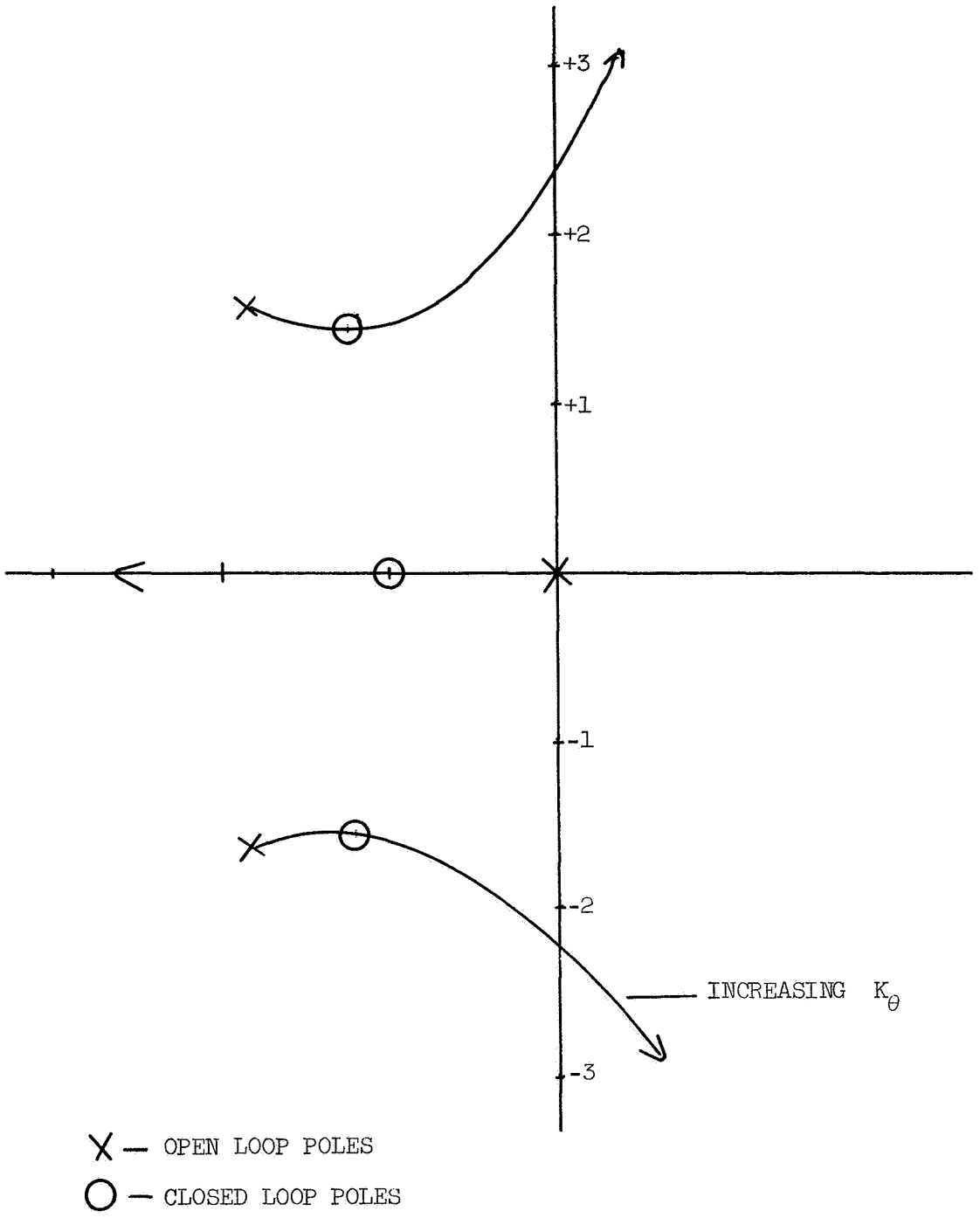

Figure 26. Root Locus.

From which,

$$\theta(t) = 1.57 - 3.03e^{-t} + 1.81e^{-1.2t} \sin(1.2t + \psi_1); \quad \psi_1 = 125^{\circ}34'$$

$$\varphi(t) = -3.03e^{-t} + 3.04e^{-1.2t} \sin(1.2t + \psi_2); \quad \psi_2 = 99^{\circ}29'$$

In the steady state, $\theta = \pi/2$. At $t = 4$ sec., $\theta = 1.52$ rad. The maximum value of φ occurs at approximately 1.17 sec. and is approximately -52°. We see that φ is relatively large, certainly out of the linear range. However, this is expected. In order to move the vehicle through 90° in four seconds, a relatively large angular velocity must be imparted to the vehicle and this is done by transferring momentum from the gyros to the vehicle. If a smaller angle φ is desired, then the gyros must have more angular momentum. However, there is no reason why φ shouldn't go as high as 60°-70°. The greater the allowable angle, the lower the required angular momentum of the gyros. In this example, the system response has been assumed very sluggish. A more realistic approach is to make the gyro response very fast and put in stops at 65-75°. With such fast response, the gyro gimbals open rapidly and hit the stops and remain there as the vehicle rotates. As θ nears θ_c, the gyros back off from the gimbals.

In the preceeding example, the torque in the gimbals is

$$T = k_\theta(\theta-\theta_c) + k_{\dot\theta}\dot\theta - b\dot\varphi$$

Presumably, the $b\dot\varphi$ torque will be produced viscously by a damper between the gimbals, so $b\dot\varphi$ will not need to be produced electrically. From the standpoint of power used in actuators, the torque of interest is

$$T = k_\theta(\theta-\theta_c) + k_{\dot\theta}\dot\theta$$

and for this example,

$$T = .953[-3.03e^{-t} + 1.81e^{-1.2t} \sin(1.2t + 2.2)$$
$$-1.98.1[3.03e^{-t} - 3.04e^{-1.2t} \sin(1.2t + 1.735)]$$

Thus at $t = 1$ sec.,

$$T = 184.19 \text{ kg } \frac{m^2}{sec^2} = 135 \text{ ft-lbs.}$$

APPENDIX H

CONTROL THEORY, LIST OF SYMBOLS

b	damping constant
c	characteristic velocity
f	thrust
g	acceleration of lunar gravity
h	angular momentum of gyro wheel
I	moment of inertia of the vehicle
J	moment of inertia of gyro wheel about a diameter
k_θ	gain in the θ-feedback loop
$k_{\dot\theta}$	gain in the $\dot\theta$-feedback loop
ℓ	center of mass to foot distance
m	mass
m_{foot}	mass of the foot
m_{gs}	mass of the gyro system
r	radius of the foot
t	time of flight
T	control torque on gyros
v	velocity of the center of mass of the vehicle

α	$\ddot\theta$
$\Delta\theta$	reorientation required about pitch between launch and landing
ΔV	velocity impulse which initiates a hop
ϵ	angle between the velocity vector and thrust leg

θ	angle between the thrust leg and the vertical
θ_c	commanded angle θ
ξ	damping ratio
σ	slope of terrain
φ	angle of gyro wheel with respect to gyro controller frame
ω	angular velocity of gyro wheel
ω_n	natural frequency